

Numerical Weather Prediction

Exploitation of Meteosat Second Generation data for volcanic ash monitoring



Forecasting Research Technical Report No. 463

Sarah C. Watkin

email: nwp_publications@metoffice.gov.uk

©Crown Copyright

A decorative wavy line that starts on the left, dips down, rises up, and then dips down again, ending on the right.

Abstract

Volcanic ash clouds threaten the safety of jet aircraft every year. The availability of operational data from Meteosat-8 (a Meteosat Second Generation (MSG) satellite) has provided an opportunity to improve the provision of satellite imagery to forecasters for the monitoring of volcanic ash and therefore improve the safety of aircraft through the Volcanic Ash Advisory Centre service.

This study investigates the application of imagery data from MSG for volcanic ash monitoring. It uses MODIS data, as a substitute for MSG data, from six recent eruptions to analyse the signal of volcanic ash. The results are compared to studies performed by others using similar data sets. It was found that the volcanic ash signal can vary greatly from one eruption to another due to factors such as: the quantity of ash, the atmospheric conditions and the viewing geometry. The commonly used split-window test (using 10.8 and 12.0 μm channels) was found to be the most reliable. However, useful information can be obtained from additional imagery. In particular, RGB imagery involving the 8.7 μm , 10.8 μm and 12.0 μm was found to highlight areas of ash.

The merits of MODIS imagery and SEVIRI imagery are discussed, and it was concluded that there is benefit in the provision of imagery for ash monitoring from both instruments. A further study into the monitoring of sulphur dioxide and investigations of future eruptions in the MSG field-of-view will add to the understanding of the spectral signature of this infrequent, but potentially dangerous, phenomenon.

Document history

Date	Version	Action/Comments	Approval
25/07/05	1.0	First draft	
02/08/05	2.0	Incorporated comments from Roger Saunders	
28/11/05	3.0	Incorporated comments from John Eyre and additional text from Roger Saunders	John Eyre

Contents

1.	The volcanic ash hazard.....	- 3 -
2.	SEVIRI on Meteosat Second Generation	- 3 -
3.	Eruptions studied	- 5 -
3.1.	Hekla, Iceland (63.98° N, 19.70° W): February 2000.....	- 5 -
3.2.	Cleveland, Alaska (52.82° N, 169.94° W): February 2001	- 5 -
3.3.	Etna, Italy (37.73° N, 15.00° E): October 2002.....	- 6 -
3.4.	Anatahan, Northern Mariana Islands (16.35° N, 145.67° E): May 2003	- 6 -
3.5.	Grímsvötn, Iceland (64.42° N, 17.33° W): November 2004	- 6 -
3.6.	Anatahan, Northern Mariana Islands (16.35° N, 145.67° E): February 2005	- 6 -
4.	Spectral features of volcanic ash and results of studies.....	- 7 -
4.1.	BT10.8 & BT12.0.....	- 8 -
4.1.1.	Results	- 8 -
4.1.2.	Comparison between MODIS and SEVIRI BT10.8 – BT12.0	- 9 -
4.1.3.	The effect of water vapour on BT10.8 – BT12.0 signal	- 10 -
4.1.4.	False alarms in BT10.8 – BT12.0 imagery	- 11 -
4.2.	BT8.7 & BT10.8 or BT12.0	- 11 -
4.3.	R0.6 & R1.6.....	- 15 -
4.4.	Visible RGB image.....	- 17 -
4.5.	Dust RGB image	- 19 -
4.6.	Other volcanic ash detection tests	- 20 -
4.6.1.	BT3.9 & BT10.8 or BT12.0.....	- 20 -
4.6.2.	Darwin VAAC BT10.8 – BT12.0 adjustment	- 20 -
4.6.3.	Ellrod 3-channel algorithm	- 20 -
5.	Conclusions and recommendations.....	- 21 -
	References.....	- 22 -
	Acknowledgments	- 22 -
	Acronyms.....	- 23 -
	Appendices	- 23 -
	Appendix A: 0.6 µm reflectance for eruption clouds (a) to (f)	- 24 -
	Appendix B: BT10.8 for eruption clouds (a) to (f)	- 25 -
	Appendix C: BT10.8 – BT12.0 for eruption clouds (a) to (f)	- 26 -
	Appendix D: BT10.8 – BT8.7 for eruption clouds (a) to (f)	- 27 -
	Appendix E: R0.6/R1.6 for eruption clouds (a) to (f)	- 28 -
	Appendix F: Visible RGB for eruption clouds (a) to (f)	- 29 -
	Appendix G: Dust RGB for eruption clouds (a) to (f)	- 30 -

1. The volcanic ash hazard

Volcanic ash in the atmosphere is a significant safety hazard for jet aircraft. It can cause engine shutdown and considerable damage to the frame of the aircraft. An average of 15-25 volcanoes erupt each year produce ash clouds that reach flight altitudes. Volcanic ash can reach cruise altitudes in 5 minutes. There are numerous instances of aircraft flying into volcanic ash clouds. Upon impact with aircraft travelling at speeds of several kilometres per minute ash particles abrade forward facing surfaces (windcreens, fuselage surfaces, compressor fan blades etc.) and, due to ash having a lower melting point than the operating temperature of jet turbine engines, particles ingested into the engine melt and then accumulate as re-solidified deposits. The overall result is to immediately degrade engine performance (in extreme cases: engine flame-out), loss of visibility and failure of crucial navigational and operational instruments. From 1973 to 2003, 105 encounters of aircraft with airborne ash have been documented (Guffanti, 2004).

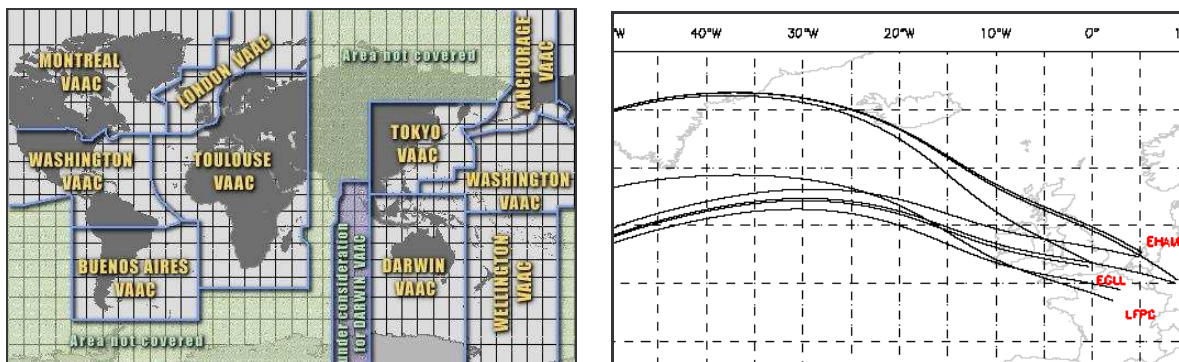


Figure 1: (a) Volcanic Ash Advisory Centre areas of responsibility. (b) Forecasted air traffic tracks at 250 hPa for a few flights on a single day.

Volcanic Ash Advisory Centres (VAACs) were established in the 1990s to issue advisories about the presence of volcanic ash in the atmosphere. The London VAAC, one of nine VAACs around the world, is operated by EMARC (Environment Monitoring and Response Centre) forecasters in the Met Office. The London VAAC area of responsibility covers the north-east Atlantic, including Iceland, where 18 volcanoes have been active since 1500 AD. The London VAAC covers part of the busy North-Atlantic air routes where 250-500 jet aircraft cross the Icelandic airspace every day (Figure 1).

2. SEVIRI on Meteosat Second Generation

The first of the new series of Meteosat Second Generation (MSG) satellites became operational in January 2004. Now renamed Meteosat-8 it has been designed to expand the services of the first Meteosat series. Positioned 36,000 km above the equator, this spin-stabilised geostationary satellite senses approximately one-quarter of the Earth every 15 minutes through its main instrument the Spinning Enhanced Visible and Infrared Imager (SEVIRI). Scanning from south to north, data over Africa, Europe and the surrounding oceans are available from 11 spectral channels at a spatial resolution of 3 km at nadir (Figure 2). In addition, SEVIRI has a high-resolution 1-km visible channel which senses a limited area of the MSG disk during daylight.

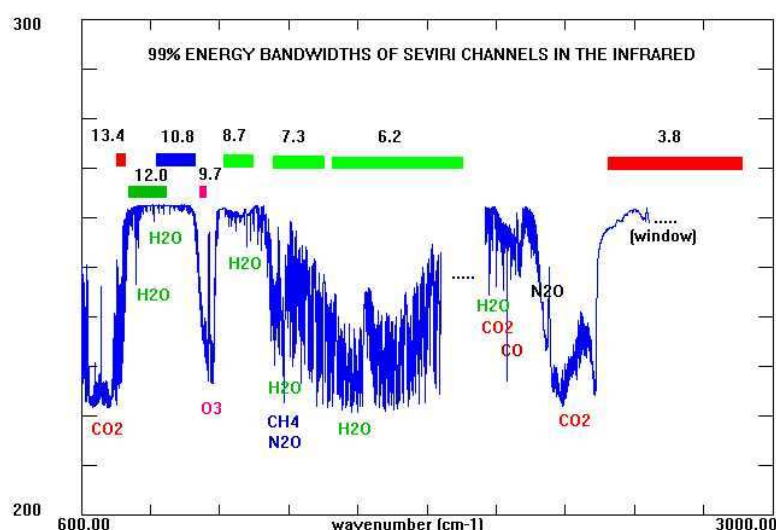


Figure 2: Infrared brightness temperatures for the range of SEVIRI wavelengths for a typical mid-latitude atmosphere. The coloured bars indicate the location of the SEVIRI channels. From EUMETSAT (http://www.eumetsat.int/en/index.html?area=left4b.html&body=/en/area4/msg/missions/211_mis_obs_spectrch.html&a=412.1&b=2&c=412&d=410&e=0).

SEVIRI data are received routinely at the Met Office in Exeter via the EUMETCAST system and are processed in near-real time by the Autosat satellite processing system to create a range of products used in operational forecasting. This paper describes the development of SEVIRI-based products to aid forecasters to track volcanic ash. It builds on previous work and experience in the development and use of a volcanic ash tracking product that uses data from the Advanced Very High Resolution Radiometer (AVHRR) (Watkin, 2001 & 2003). A comparison of imagery from SEVIRI, AVHRR and MODIS is shown in Table 1. While, SEVIRI can provide imagery at a high temporal coverage, AVHRR can provide imagery at higher spatial resolution at the high latitudes of Iceland and the North Atlantic.

	SEVIRI (on Meteosat-8 geostationary satellite)	AVHRR (on NOAA polar satellites)	MODIS (on TERRA and AQUA polar orbiting platforms)
Web reference	http://www.eumetsat.int/en/area4/topic1.html	http://www.oso.noaa.gov/poes/	http://modis.gsfc.nasa.gov/
Temporal coverage	Every 15 minutes	Approx. 12-14 per day for Iceland	Approx. 8 per day over Iceland.
Spatial coverage	Full-earth disk (up to 70° N) at 3 km resolution sub-satellite point (increases to approx. 11km over Iceland)	Global at 1 km resolution at sub-satellite point. Only local area data are received.	Global at 1 km resolution at sub-satellite point (down to 250 m for a few visible channels). Only local area received.
Areas covered by current volcanic ash imagery	London VAAC area, Mediterranean area, Central Africa and the Caribbean	London VAAC area and Mediterranean area	London VAAC area and Mediterranean area

Table 1: Comparison between SEVIRI, AVHRR and MODIS data.

In order to obtain a number of case studies of volcanic eruptions it was necessary to use satellite data from an instrument with a longer operational history than SEVIRI. The Moderate Resolution Imaging Spectroradiometer (MODIS) has 36 spectral bands, some of which closely match the central wavelength of SEVIRI channels (Table 2). MODIS channels are much narrower than those on SEVIRI, however the channels are sufficiently similar to enable studies to be carried out using MODIS data as a substitute for SEVIRI data. The MODIS instrument is carried on the Terra and Aqua polar orbiting satellites.

SEVIRI channel	SEVIRI bandwidth (μm)	MODIS channel number	MODIS bandwidth (μm)
VIS0.6	0.56-0.71	1	0.620-0.670
VIS0.8	0.74-0.88	2	0.841-0.876
NIR1.6	1.50-1.78	6	1.628-1.652
IR3.9	3.48-4.36	20	3.66-3.84
IR6.2	5.35-7.15	27	6.535-6.895
IR7.3	6.85-7.85	28	7.175-7.475
IR8.7	8.30-9.10	29	8.400-8.700
IR9.7	9.38-9.94	30	9.580-9.880
IR10.8	9.80-11.80	31	10.780-11.280
IR12.0	11.0-13.00	32	11.770-12.270
IR13.4	12.40-14.40	33	13.185-13.485

Table 2: SEVIRI channels and the MODIS channel substitutes used in this study.

3. Eruptions studied

Volcanic ash detection tests were studied using MODIS imagery of six recent eruptions. A brief overview of each of the eruptions is given below.

3.1. Hekla, Iceland (63.98° N, 19.70° W): February 2000

Hekla started erupting from a 6-7 km long fissure at 1819 UTC on 26 February 2000. The eruption produced a volcanic cloud that was reported to have risen to an altitude of 11 km in only 6 minutes (Smithsonian Institution, Global Volcanism Program). The eruption continued sporadically until 29 February 2000. Met Office forecasters operating the London VAAC service issued over 15 volcanic ash advisory statements during the course of the eruption and during the dispersal of the volcanic cloud. Ash fall was reported on 26 February from Grimsey Island, approximately 300 km north of Hekla. Although small amounts of ash fell in inhabited areas of northern Iceland, most fell in uninhabited areas of the interior. Seven hours after the eruption's onset an ash deposit 21 km north of Hekla had a maximum thickness of 4-5 cm.

Imagery from the Earth Probe TOMS (Total Ozone Mapping Spectrometer) instrument shows a narrow plume of sulphur dioxide (SO₂) arcing from the volcano in southern Iceland, then north to Greenland, and finally east towards Norway at 1154 UTC on 27 February. Observations also came from a DC-8 aircraft which was carrying out measurements for a SOLVE (SAGE III Ozone Loss and Validation Experiment) mission. It inadvertently flew through the plume on 28 February, approximately 1400 km north of Hekla, and reported that the plume extended up to approximately 13 km altitude (Gridle and Burcham, 2003). On 29 February the SOLVE aircraft again entered the volcanic cloud. The scientific team reported large enhancements in H₂O, CN, NO_y, HNO₃, CO, and particle counts, while ozone measurements went to nearly zero (Smithsonian Institution, Global Volcanism Program). They reported strong scattering layers up to 13 km and that the plume was a very impressive, orange, airfoil-shaped feature in the pre-dawn sky. During the three weeks following the initial encounter the DC-8 detected remnants of the plume trapped within the polar vortex. The resulting analysis concluded that volatile aerosols increased and the sizes of non-volatile large aerosols decreased. Inspections showed that there was damage to the engines of the DC-8 aircraft during the flights before, during or after the encounter with the Hekla emissions. This eruption has been the subject of considerable debate about whether volcanic ash particles were present in the path of the DC-8 aircraft and if so, some argue that this is evidence that weak volcanic ash clouds can cause damage to aircraft.

3.2. Cleveland, Alaska (52.82° N, 169.94° W): February 2001

The eruption began at approximately 1400 UTC (0600 local time) and continued for at least eight hours, ending between 2230 and 0242 UTC (Dean et al., 2004). The eruption on this remote island was detected using satellite imagery at the Alaska Volcano Observatory. Pilot reports later indicated that the altitude of the

eruptive cloud increased with time from 7.5 km just after the start of the eruption to 12 km eight hours later. There was significant wind shear which split the plume: below approximately 6 km the plume moved in a south-easterly direction and above in a north-westerly direction. Ash fall was reported on the island of Nikolski, 72 km to the east and the plume was tracked for 48 hours using satellite imagery as it moved towards and over mainland Alaska (Figure 3).

3.3. *Etna, Italy (37.73° N, 15.00° E): October 2002*

The eruption started early on 27 October 2002 from two fissures on north-east and southern flanks. The highly explosive eruption caused the international airport at Catania to be closed for two weeks due to airborne ash and ash on runways. The eruption continued until 28 January 2003. At the start of the eruption, the ash cloud reached more than 5 km in altitude. It dispersed in a south-easterly direction.

3.4. *Anatahan, Northern Mariana Islands (16.35° N, 145.67° E): May 2003*

The explosive eruption which began on 10 May 2003 was the first documented eruption from Anatahan in historical times. The eruption began at approximately 0700 UTC and the plume reached an estimated altitude of 10.5 km by 1230 UTC on 10 May. One layer of the ash cloud drifted south at a speed of ~65 km/hour, and at an altitude of ~4.5 km a second layer of ash drifted west at ~28 km/hr. By 2055 UTC ash was seen in satellite imagery drifting in three different directions: WNW at an altitude around 5.5 km, SW around 8.5 km, and two separate and smaller ash plumes were drifting SE at altitudes around 13.4 km. The eruption continued until at least 14 May. The TOMS data on 12 May at 0115 UTC revealed an ash cloud extending ~560 km on its long axis centred ~570 km west of Anatahan and an SO₂ cloud, again displaced from the ash, extended ~1,100 km from a point ~510 km west of the volcano to a point ~700 km south-east of it - this cloud contained ~110 kt of SO₂ (Smithsonian Institution, Global Volcanism Program).

3.5. *Grímsvötn, Iceland (64.42° N, 17.33° W): November 2004*

Grímsvötn volcano erupted in the evening of 01 November 2004. The Icelandic Meteorological Office gave pre-eruptive notice to the Met Office of the increase in seismic activity. At approximately 2300 UTC the eruption broke through the Vatnajökull ice cap. Radar data shows that the eruption cloud reached 13 km by 0235 UTC. Met Office forecasters issued Volcanic Ash Advisory Statements throughout the eruption using information supplied by Icelandic Met Office and NAME dispersion model output. Observations also came from pilots over Scandinavia and satellite imagery. Over 100 flights had to be cancelled and many flights diverted.

3.6. *Anatahan, Northern Mariana Islands (16.35° N, 145.67° E): February 2005*

Anatahan's third historical eruption began on 5 January 2005. Eruptions continued until at least 18 February 2005. This eruption caused disruption to flights as aircraft were advised to avoid the area within 30 km downwind of Anatahan. The volcanic haze spread throughout the region as the eruption persisted and air quality in Guam, 320 km south of the volcano, deteriorated to such an extent that school children were sent home suffering from dizziness or nausea.

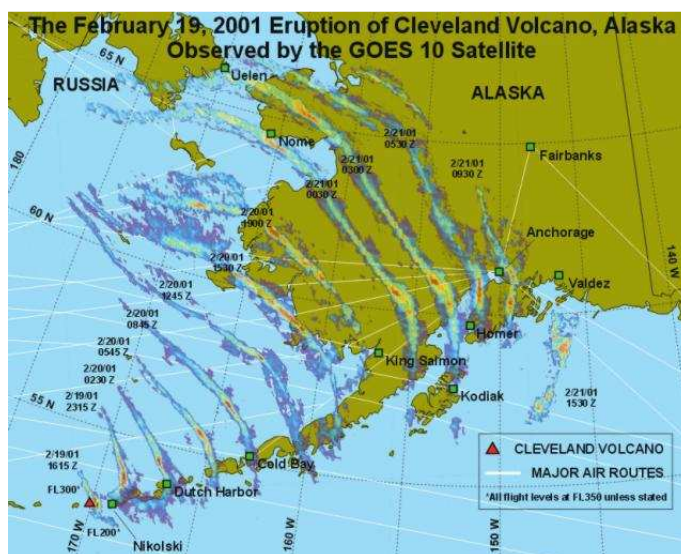


Figure 3: Composite of GOES BT10.8 – BT12.0 images showing the progressive locations and evolution of the ash clouds erupted from Cleveland during 19-21 February 2001. Blue to red colours show negative values increasing in magnitude. From Alaska Volcano Observatory.

4. Spectral features of volcanic ash and results of studies

Volcanic ash particles are fragments of rock ejected from a volcano during an eruption. The nature of the volcano in terms of the composition of the ejected magma and the ferocity of the eruption affect the properties of the volcanic ash particles. Moreover, once the ash forms a cloud in the atmosphere its properties can change: the larger particles fall out, water vapour is convectively lifted with the ash and ice crystals can form around the fine ash particles. The silicates in volcanic ash particles possess absorption characteristics that enable spectral techniques to be used to differentiate volcanic ash from water or ice clouds. Figure 4 shows the spectral response functions of the MODIS and SEVIRI instruments alongside the transmission spectra for some common components of volcanic clouds.

Several meteorological and/or vulcanological centres have carried out studies to investigate the spectral signature of volcanic ash clouds in satellite imagery from a variety of instruments. These instruments (e.g. GOES imager, AVHRR, MODIS) have channels with central wavelengths that are similar to some of those on SEVIRI. Therefore, many of the findings can be applied to SEVIRI data.

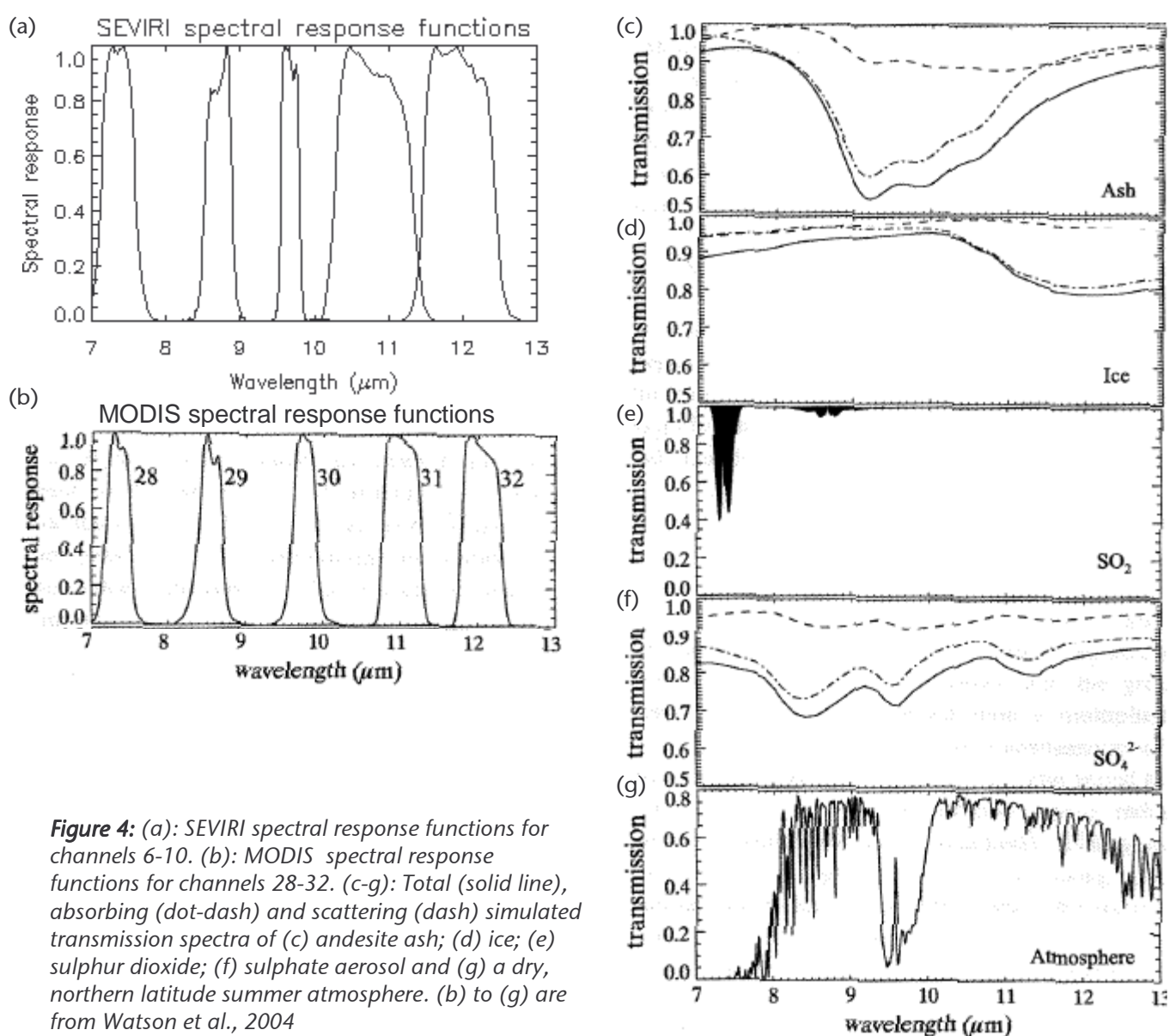


Figure 4: (a): SEVIRI spectral response functions for channels 6-10. (b): MODIS spectral response functions for channels 28-32. (c-g): Total (solid line), absorbing (dot-dash) and scattering (dash) simulated transmission spectra of (c) andesite ash; (d) ice; (e) sulphur dioxide; (f) sulphate aerosol and (g) a dry, northern latitude summer atmosphere. (b) to (g) are from Watson et al., 2004

In the following sections are descriptions of the application of data from SEVIRI channels for volcanic ash tracking, mainly using MODIS data as a substitute. Mostly, pairs of channels are used to look at the brightness temperature (BT) difference or reflectance (R) ratio. The convention used here is that the central wavelength of the channel is given in microns after the BT or R, e.g. BT10.8 is the brightness temperature at

10.8 μm and R0.6 is the reflectance at 0.6 μm . The images of the six eruptions studied (and described in section 3) are shown in the Appendices.

4.1. **BT10.8 & BT12.0**

The application of data from the split-window channels (BT10.8 & BT12.0) to detect volcanic ash is a well-established method (Watkin, 2001 & 2003). Volcanic ash particles are rich in silica and exhibit stronger absorption at the longer wavelengths in the 10-12 μm atmospheric window than the shorter wavelengths (Figure 4c). These absorption characteristics are the reverse to those for water vapour and water or ice clouds. Prata (1989) describes a method using AVHRR data to discriminate between volcanic ash clouds and water or ice clouds. Typically, the difference between the brightness temperature at 10.8 μm (BT10.8) and the brightness temperature at 12.0 μm (BT12.0) is negative when volcanic ash is present in the atmosphere and positive when water or ice is present in the atmosphere.

In addition to the variation of optical properties of volcanic ash, the surface and atmospheric optical effects on the signal can be strong, affecting the performance of this detection method. These factors are described by Watkin (2003). Many studies have since been conducted using this technique to observe volcanic ash (e.g. Rose and Mayberry, 2000; Constantine et al., 2000; Schneider et al., 1999; Rose et al., 1995).

4.1.1. Results

Volcano		Approximate measured BT10.8 – BT12.0 values
(a)	Hekla	+0.5 K: Clear sky
(b)	Cleveland	-8 to -1 K: Volcanic plume +1 K: Clear sky
(c)	Etna	-4 to -1 K: Volcanic plume +1 K: Clear sky
(d)	Anatahan	-2.5 to +1 K: Volcanic plume +1.5 K: Clear sky
(e)	Grímsvötn	-1 to +1 K: Volcanic plume + 0.5 K: Clear sky
(f)	Anatahan	-1 to +1 K: Volcanic plume +1 K: Clear sky

Table 3: Approximate observed signals in the imagery shown in Appendix C.

Negative BTDs (brightness temperature differences) are seen here for all the volcanic plumes except for the Hekla eruption (although we cannot be sure where the volcanic ash is, if there is any). The eruptions of Cleveland, Etna and Anatahan in 2003 produced volcanic clouds that gave particularly strong BTD signals. The Cleveland volcanic plume rose to an altitude of 12 km, well into the stratosphere. The plume would have contained little water vapour and with negligible water vapour in the atmosphere above the volcanic plume there was a strong ash signal that was not dampened by water vapour absorption. The Etna and Anatahan eruptions produced a large volume of volcanic ash resulting in a coherent negative BTD signal. However, high clear sky BTDs resulted in the volcanic ash signal being reduced due to the increased absorption of the 12.0 μm radiation by water vapour (see Figure 7 and accompanying text). Water vapour has almost completely masked the volcanic cloud from the 2005 Anatahan eruption.

The volcanic plume from the eruption of Grímsvötn does not produce a coherent negative signal and therefore the plume cannot be identified in this image. This may be because: there was very little ash (although ash fall was reported), that the ash was coated in ice (quite likely), that the volcanic cloud is optically thick (but should see negative values along the semi-transparent edges) or some other reason. Most likely, the plume contained some ash and some ice-coated ash. There was also an inhomogeneous surface signal due to varying emissivity properties that added to the complexity of the observed BTDs (there is a large ice cap, barren land, vegetation and ocean).

4.1.2. Comparison between MODIS and SEVIRI BT10.8 – BT12.0

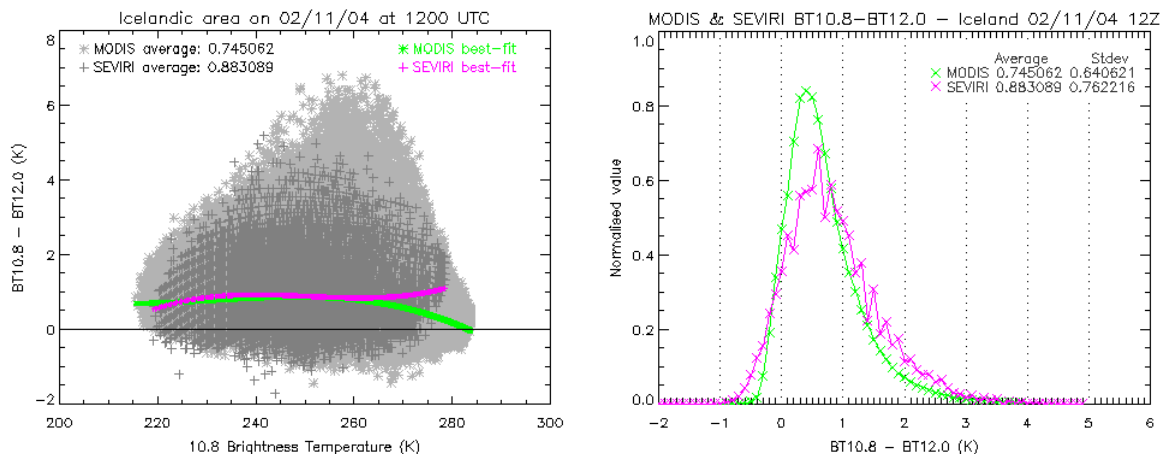


Figure 5: Comparison between MODIS and SEVIRI BT10.8 – BT12.0 values for the Icelandic region during the Grímsvötn eruption on 02/11/04 (the volcanic signal is negligible). MODIS data were from Terra at 1210 UTC and the SEVIRI data were measured at approx. 1155 UTC.

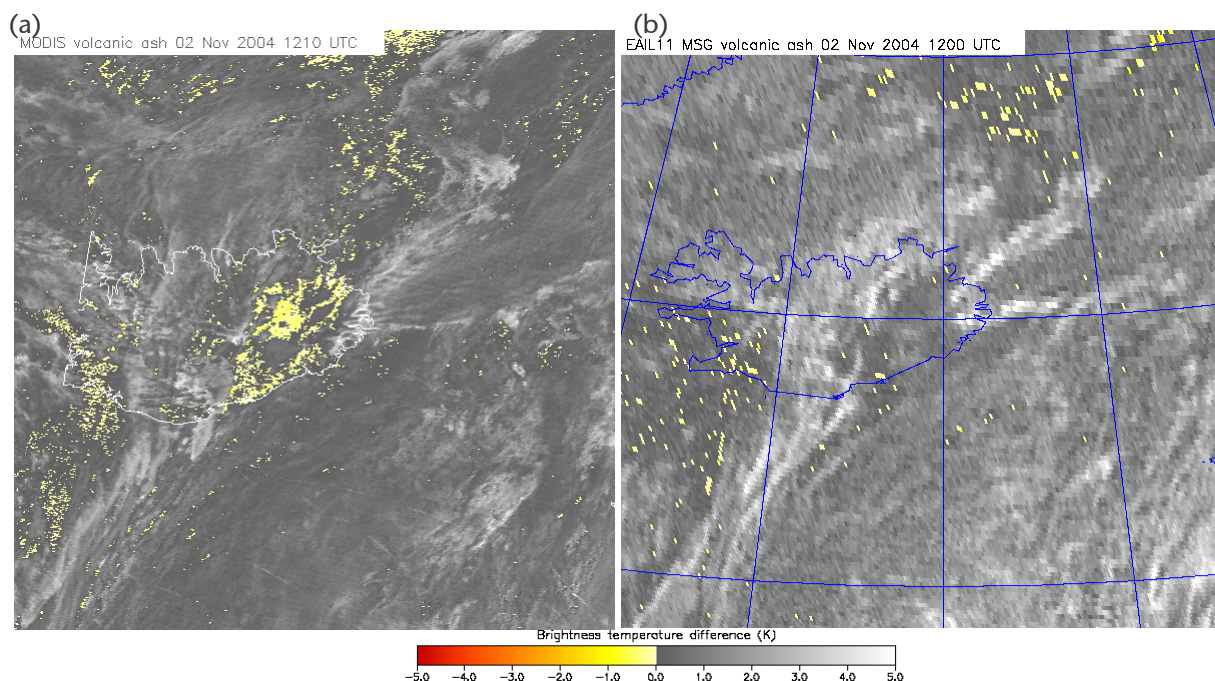


Figure 6: (a) A MODIS BT10.8 – BT12.0 image and (b) the corresponding SEVIRI BT10.8 – BT12.0 image at approximately 1155 UTC on 02/11/04.

The effect of the increased water vapour absorption at 12.0 μm along the longer path length for SEVIRI measurements compared to MODIS due to the viewing geometry can be seen in Figures 5 and 6. The clear-sky BTD is positive for SEVIRI (approximately 1 K) and zero or negative for MODIS. The negative pixels in Figure 6a are mainly over the Vatnajökull glacier and are probably caused by the directional emission properties of the ice surface. However, the cloudy measurements (both semi-transparent and opaque) are similar from both instruments. This leads to the conclusion that we can expect a volcanic ash cloud to produce a similar signal in MODIS and SEVIRI imagery. The main difference is in the spatial resolution of the data: MODIS imagery will display far greater detail than SEVIRI imagery, especially at Icelandic latitudes, as demonstrated by Figure 6.

4.1.3. The effect of water vapour on BT10.8 – BT12.0 signal

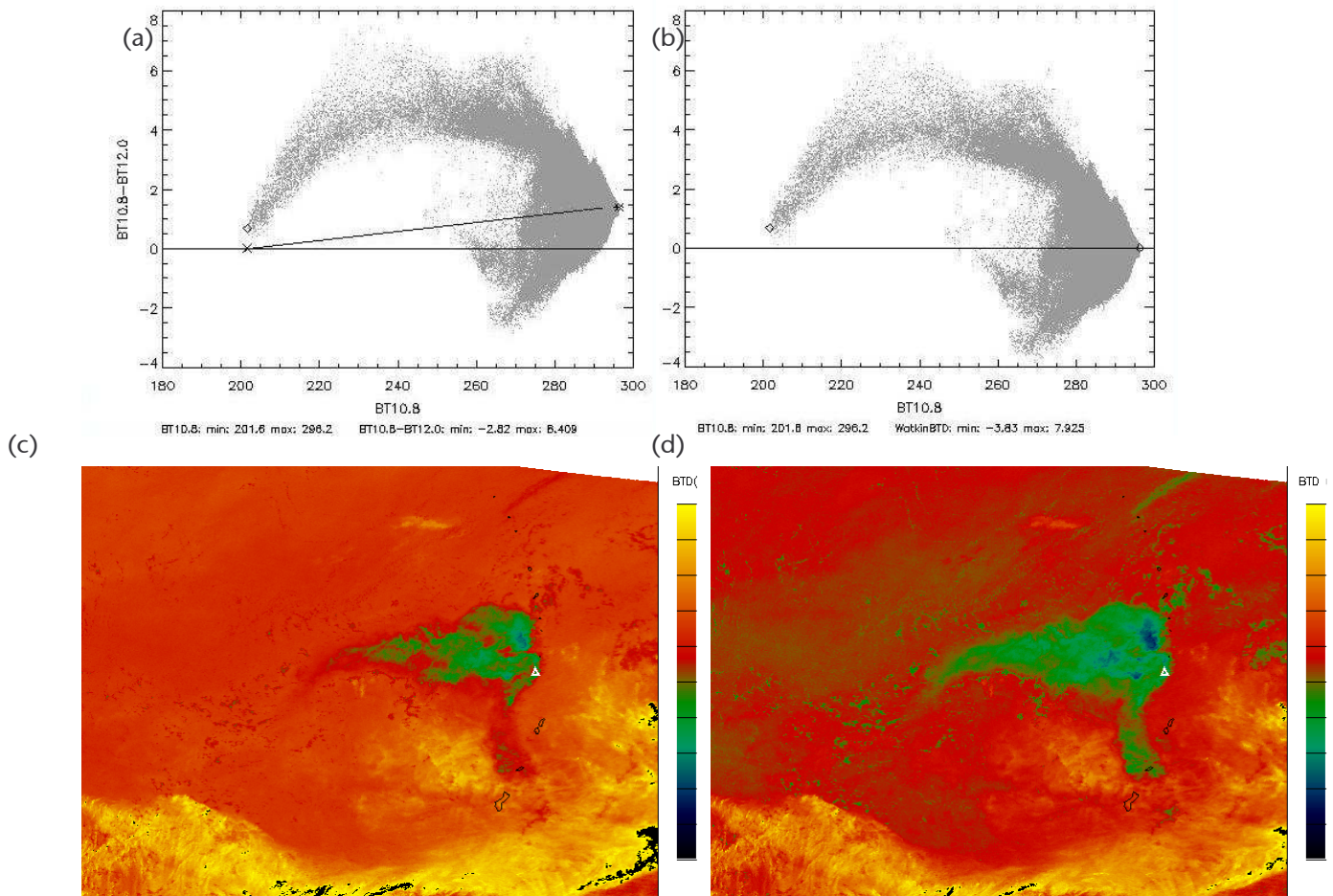


Figure 7: MODIS BT10.8 – BT12.0 data for the Anatahan eruption on 11 May 2003 at 0125 UTC. (a) and (c) show a scatter plot and image of measured BT10.8 – BT12.0 values, (b) and (d) show a scatter plot and image of water-vapour adjusted BT10.8 – BT12.0 values.

Water vapour absorption is greater at 12.0 μm than at 10.8 μm resulting in a positive BTD signal. In humid regions the water vapour signal can significantly reduce the observed region of volcanic ash and can mask the signal completely. The eruption of Anatahan in 2003 produced a large ash cloud that was significantly masked by water vapour. A method to adjust the measured signal for water vapour absorption and therefore reveal the complete ash cloud was developed.

Within a region around the volcano ($\pm 5^\circ$) the maximum 10.8 μm brightness temperature is found – this is assumed to be a clear sky pixel. The BTD at this pixel is taken to be representative of the clear sky BTD and consists largely of a water vapour signal. The equation of a straight line is calculated between the clear sky BTD at the corresponding 10.8 μm BT and a zero BTD at the coldest (assumed opaque) cloud within the same area. This line is plotted for the Anatahan example in Figure 7a. All pixels are then adjusted for the clear-sky (mainly water vapour) signal by moving the plotted line to zero BTD (i.e. subtracting the clear-sky signal from the measured signal). The resultant image reveals a much increased area of volcanic ash (Figure 7d). A curved rather than a straight line would make a more accurate adjustment; however a straight line adjustment should, and does, result in an improvement.

This adjustment should only be made to regions in the tropics since the higher latitudes tend to have lower total column water vapour amounts and therefore the BT10.8 – BT12.0 signal is not affected to the same degree. If the adjustment is applied to the Icelandic image, large areas of water cloud are shown to have negative BTDs.

4.1.4. False alarms in BT10.8 – BT12.0 imagery

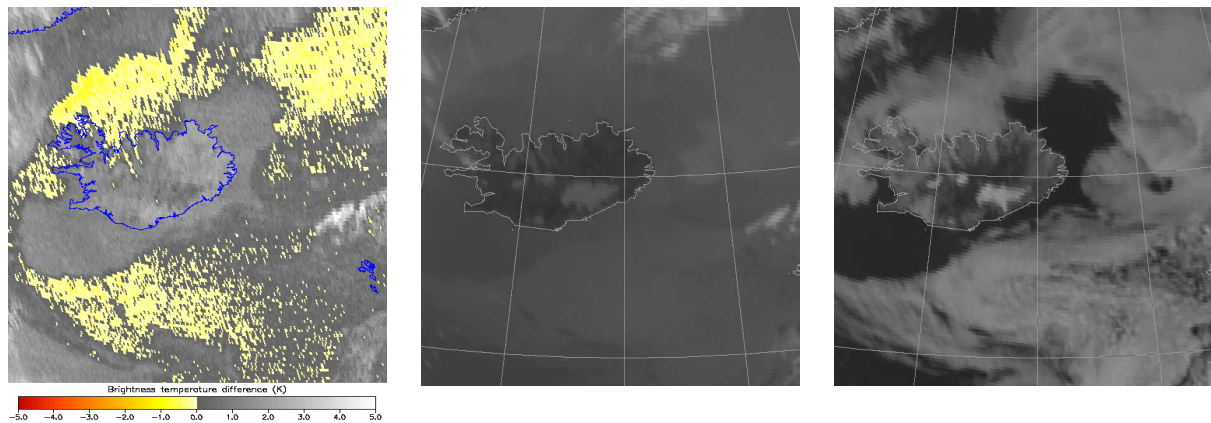


Figure 8: SEVIRI BT10.8 – BT12.0, infrared and visible images of Iceland at 0845 UTC on 14 July 2005.

Negative BT10.8 – BT12.0 values frequently occur. The causes of these false ash signals are not wholly understood. Some common situations are:

- Desert dust: Only really a problem close to deserts (e.g. Mediterranean) and can usually be tracked back to their source.
- Channel misalignment: The slightly different fields of view between the 10.8 and 12.0 μm channels can cause negative (and positive) signals in highly inhomogeneous regions (e.g. edges of small convective clouds). The speckled pattern is easily recognised and cannot be confused with an ash cloud. In principle, this effect can be minimised by correcting the measured signal for the known misalignment error.
- Non-vegetative surfaces: Desert and ice surfaces can produce negative signals due to the emissivity properties (i.e. more emissive at 12.0 than at 10.8 μm). Ice surfaces have directionally varying emissivity properties and so the signal seen depends on the satellite viewing angle.
- Low level temperature inversions: When the air temperature is greater than the surface temperature negative BTDs can occur due to the greater emission at 12.0 μm from the warm air than at 10.8 μm .
- Opaque cloud: In the upper troposphere and stratosphere there is very little water vapour, so the signal is dominated by gaseous absorption. This is greater at 10.8 μm than at 12.0 μm resulting in a negative signal over opaque clouds in certain atmospheric conditions. The different signals in the 10.8 and 12.0 μm channels may also be caused by the microphysical properties of the ice crystals.
- High latitude fog / low cloud: Frequently, negative signals are observed in the Iceland region associated with low cloud (e.g. Figure 8) and occasionally clear sky. The BTDs are always small (-0.1 to -0.5 K), and are probably caused by the lack of water vapour absorption in the dry atmosphere above the cloud layer.

4.2. BT8.7 & BT10.8 or BT12.0

The 8.7 μm channel is sensitive to sulphur dioxide and sulphuric acid aerosol as well as volcanic ash (Figure 4). The transmission spectra computed by Watson et al. (2004) show that the transmission through andesite ash varies greatly in the SEVIRI and MODIS channels centred at 8.7 μm . The graphs show that the signal in the presence of andesite ash is similar in the 8.7 and 10.8 μm MODIS channels and slightly greater in the 12.0 μm channel, whilst sulphur dioxide is more absorbing at 8.7 μm than in the split-window channels.

Baran et al. (1993) studied volcanic aerosol from the 1991 Pinatubo eruption using HIRS (High-resolution Infra-Red Sounder) data. Transmission spectra based on in-situ observations show a distinct minima at 8.2 μm for sulphuric acid aerosol and slight minima at approximately 10 μm for volcanic ash aerosol (Figure 9). Based on these results, the proportion of volcanic ash to sulphuric acid aerosol would determine the sign of BT10.8 – BT8.7. Using the observation data collected, Baran et al. (1993) found that BT8.2 – BT12.0 gave a value of -0.04 K for volcanic ash (and Figure 9 indicates that BT8.7 – BT10.8 would be positive for volcanic ash). However, Prata and Grant (2001) modelled the expected BT8.5 – BT12.0 for andesite volcanic ash particles and predicted that they cause a large negative BTD (Figure 10).

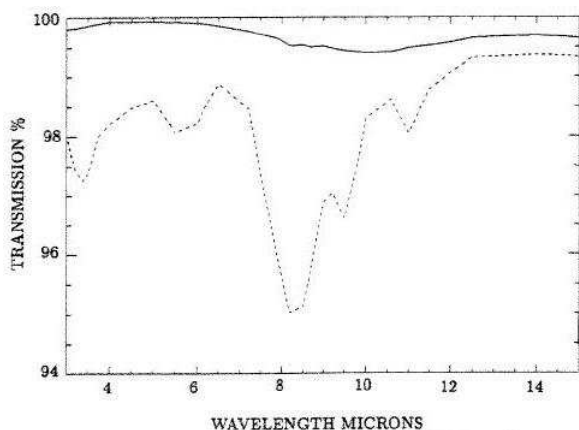


Figure 9: Calculated spectral transmission based on in-situ observations for volcanic ash (solid line) and sulphuric acid aerosol (dashed line). From Baran et al. (1993).

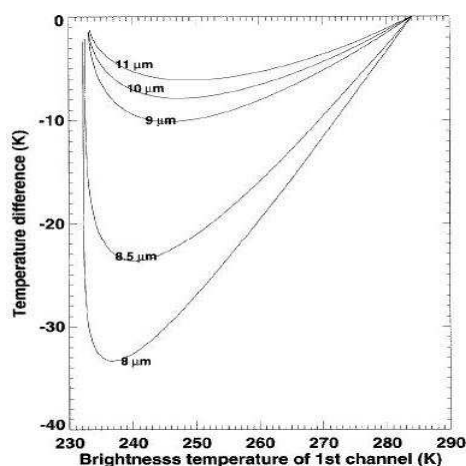


Figure 10: Brightness temperature difference vs. BT curves for combinations of infrared channels with 12 µm channel as the reference channel. Calculations were performed using the discrete-ordinates radiative transfer model and optical properties of an idealised andesite (volcanic ash) cloud. From Prata and Grant (2001).

Observations using the 8.7 µm channel have produced a variety of results, possibly because the volcanic clouds contain varying proportions of volcanic ash, sulphur dioxide and sulphuric acid aerosol. Ellrod and Im (2003) found that the volcanic cloud from the 2001 Cleveland eruption produced BT8.7 – BT12.0 values of -6 to -15 K and water and ice clouds produced values of 0 to +6 K. The Nowcasting Satellite Application Facility (Le Gléau, 2001) found that whilst volcanic cloud from Sheveluch, Russia, produced negative BT8.7 - BT10.8 values, the volcanic cloud from the 2001 eruption of Etna caused positive BT8.7 - BT10.8 values

Volcano		Approximate measured BT10.8 – BT8.7 values	
(a)	Hekla	+3 K:	Clear sky value:
(b)	Cleveland	-2 K:	Opaque plume near volcano (altitude 1.7 – 7.5 km)
		+8 K:	Dispersed plume (altitude up to 12 km, i.e. stratosphere)
		+2 K:	Clear sky
(c)	Etna	-1 to -3 K:	Thick plume
		+1 K:	Semi-transparent plume
		+3 to +4 K:	Clear sky
(d)	Anatahan	-1 to -2 K:	Sections of plume, particularly near to volcano (not opaque)
		+2 to +4 K:	Thinner sections of the plume, dispersed.
		+2.5 K:	Clear sky
(e)	Grímsvötn	+2 to +3 K:	Main dispersed plume
		+1 K:	Clear sky
(f)	Anatahan	+2 K:	plume (cannot be distinguished from background)
		+2 to +3 K:	Clear sky

Table 4: Approximate observed signals in the imagery shown in Appendix D.

Volcanic clouds result in a variety of BT10.8 – BT8.7 signals depending on its thickness and composition. A contribution to the variability is due to the relative quantities of volcanic ash and sulphur dioxide. If volcanic ash dominates a negative BTD is observed, and if sulphur dioxide dominates a positive BTD is observed. However, there are some confusing signals. For example, the Cleveland plume shows a clear volcanic ash signal in BT10.8 – BT12.0 imagery and in BT10.8 – BT8.7 imagery the plume contains both negative and positive BTDs. The negative signal occurs when the plume is more absorbing at 10.8 µm than at 8.7 µm, disagreeing with Prata and Grant (2001), but agreeing with Baran et al. (1993). The sign of the BT10.8-BT8.7 signal may also switch as the volcanic plume crosses the tropopause, so that a plume with a negative signal in the troposphere will have a positive signal in the stratosphere due to the reversal of the temperature profile (this may be the cause of the sign reversal for the Cleveland plume (Figure 13)). The variety of signals agrees with those studied within the Nowcasting SAF. Since we do not know the composition of the volcanic clouds, we cannot be sure if the absorption at 8.7 µm and 10.8 µm is due to water vapour, volcanic ash, sulphur dioxide or sulphuric acid aerosol, or, most likely, a mixture of these. The

ratio of constituents in the volcanic plume may explain why a strong volcanic ash signal may be seen in BT10.8 – BT12.0 imagery and a weak signal in BT10.8 – BT8.7 imagery.

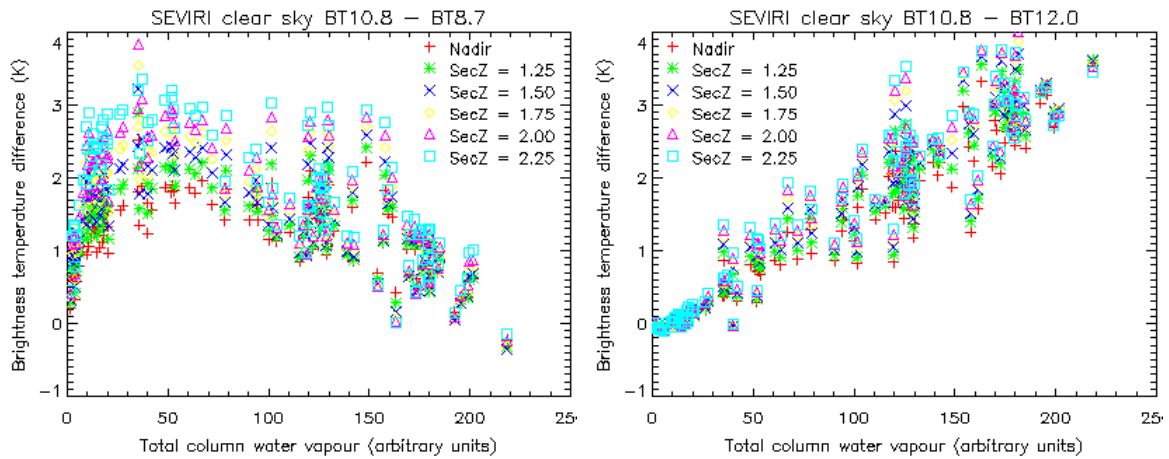


Figure 11a: RTTOV clear sky simulations of SEVIRI brightness temperatures at various viewing angles (Z) for a set of 117 diverse profiles.

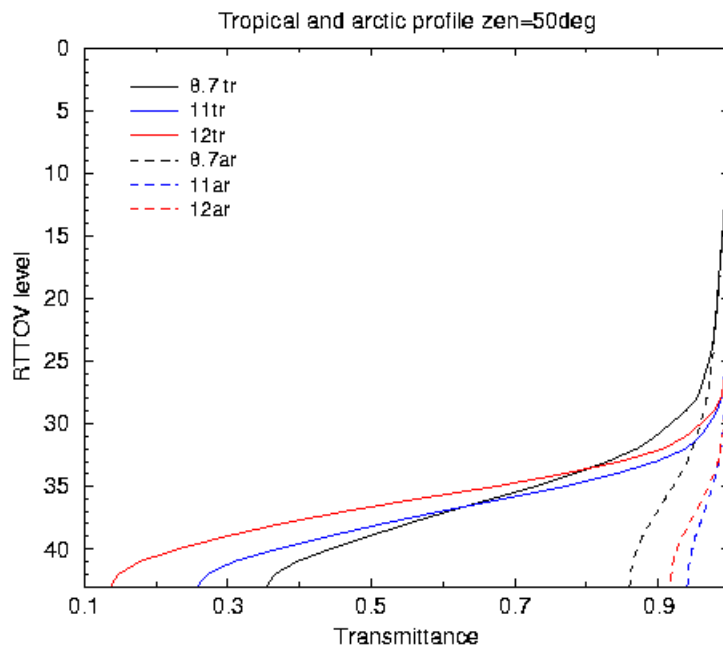


Figure 11b: RTTOV clear sky simulations of SEVIRI transmittances for a typical tropical profile (tr) and a typical arctic profile (ar). Transmittance profiles are plotted against RTTOV vertical level (level 1 = highest level, 43 = lowest level) for a viewing angle of 50° .

Thick water or ice clouds tend to have negative values (-1 to -4 K) due to gaseous absorption at 10.8 μm above the cloud top (Appendix 4). Low level water clouds have positive values, similar to clear sky values (+1 to +4 K). This is due to greater water vapour absorption at 8.7 μm than at 10.8 μm . The clear sky signal is strongly dependant on surface emissivity and the total column water vapour. It can be seen from Figure 11a that in relatively dry atmospheres the BTD increases with total column water vapour and for moist atmospheres the BTD decreases with total column water vapour. In contrast, the BT10.8 – BT12.0 increases linearly with total column water vapour. The reason for this behaviour is that the 8.7 μm channel has a few strong water vapour and ozone lines within the channel whereas the 11 and 12 μm channels do not. The result of this is that the transmittances at high level are significantly less at 8.7 μm (see Figure 11b). For cold dry atmospheres the surface emission dominates in all channels and so the effect of water vapour is linear for channel differences. For warm moist atmospheres the lack of weak water vapour lines at 8.7 μm results in the transmittance for this channel being higher than at 11 and 12 μm and so it 'sees' more of the warm surface. However when radiances (or BTs) are considered, the effect of the strong lines in the 8.7 μm band offsets this warming resulting in the BTs being similar as shown in Figure 11a. The tropical location of

Anatahan means that the total column water vapour is relatively high, resulting in a fairly large clear-sky BT10.8 - BT12.0 value (+1.5 K) and a BT10.8 – BT8.7 value of +2.5 K. However, in the region of Etna the lower total water vapour content results in a lower clear-sky BT10.8 - BT12.0 value (+1.0 K) and a higher BT10.8 – BT8.7 value (+4 K).

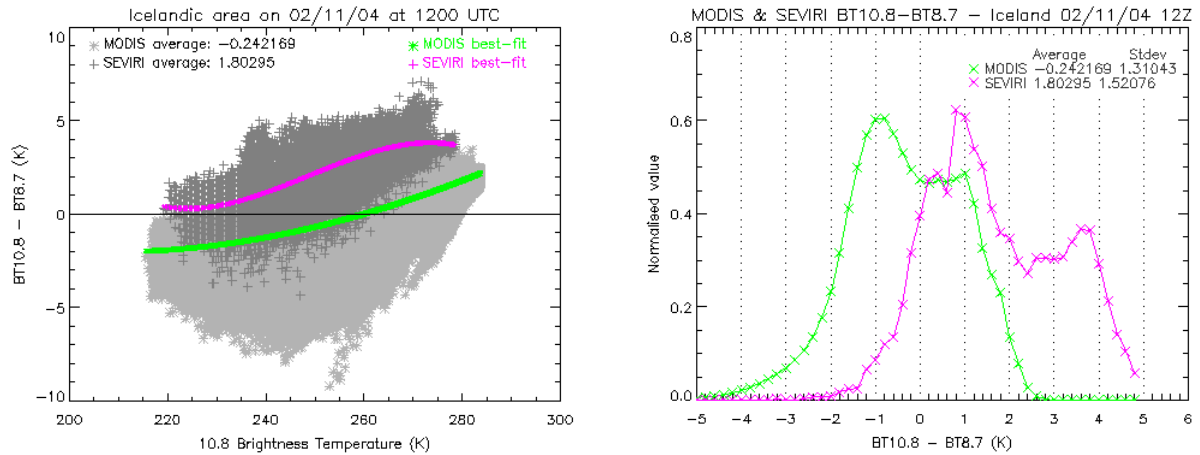


Figure 12: Comparison between MODIS and SEVIRI BT10.8 – BT8.7 values for the Icelandic region during the Grímsvötn eruption on 02/11/04 (although the volcanic signal is negligible). MODIS data were from Terra at 1210 UTC and the SEVIRI data were measured at approx. 1155 UTC. The viewing angle over central Iceland for the MODIS instrument was approximately 25° and for SEVIRI was approximately 70°.

The effect of water vapour absorption due the longer atmospheric path length for the SEVIRI observations can be seen in Figure 12. Here, the greater effect of water vapour absorption in the SEVIRI 8.7 µm channel results in a positive bias compared with the MODIS BTD.

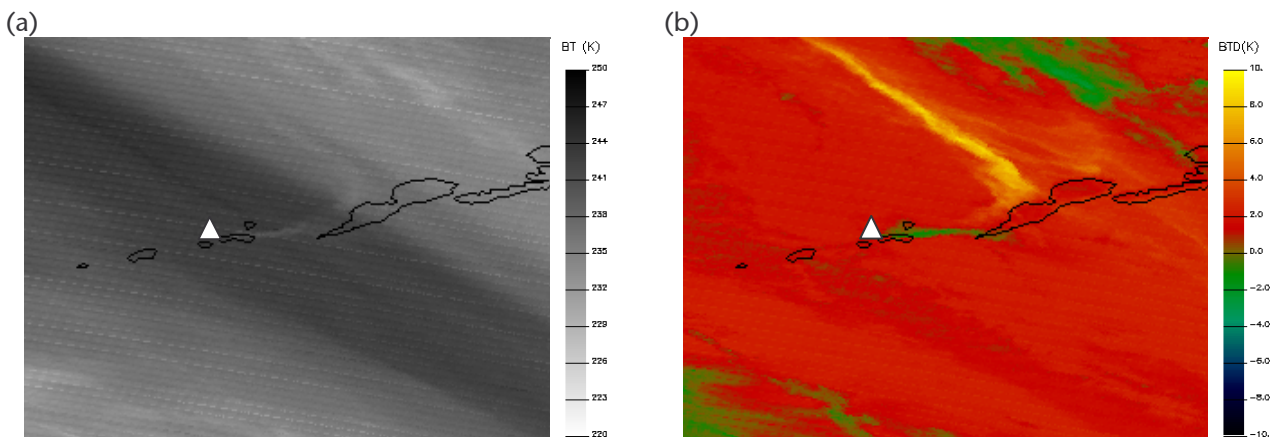


Figure 13: MODIS images of the Cleveland eruption on 19/02/01 at 2310 UTC. (a) 6.2 µm water vapour image and (b) BT10.8 – BT8.7 brightness temperature difference image. The location of the volcano is shown by the white triangle.

Figure 13 shows the eruption of Cleveland in February 2001 which occurred into a particularly dry air mass, as can be seen in the 6.2 µm image. The volcanic plume rose with little entrainment of tropospheric water. While in the troposphere, the BT10.8 – BT8.7 values are negative. The higher altitude plume aligned SE to NW has positive BTDs; this plume is likely to be in the upper troposphere or lower stratosphere, above the main water vapour layer. It is hypothesised that the two parts of the plume result in a different signal due to the age and composition of the plume. The “young” plume (near the volcano) is dominated by volcanic ash and hence generates a negative BT10.8 – BT8.7 signal due to greater absorption at 10–12 µm than 8.7 µm; as shown by Baran et al. (1993). The “older” plume contains ash (as shown by the negative BT10.8 – BT12.0 signal) and possibly sulphuric acid aerosol generated from the reaction of sulphur dioxide and water vapour. The sulphuric acid aerosol absorbs more radiation in the 8.7 µm channel than the 10.8 µm channel (see Figure 9) resulting in a positive BT10.8 – BT8.7 signal.

4.3. R0.6 & R1.6

The application of visible and near-infrared reflectances to volcanic ash detection complements the application of data at thermal infrared wavelengths because the strongest signal occurs when a volcanic ash cloud is optically thick which is often when thermal infrared methods fail. The disadvantage is that it can only be used during daylight hours.

	Wavelength (μm)	n_r	n_i
Ice	0.63	1.309	1.04×10^{-8}
	1.61	1.289	3.41×10^{-4}
Water	0.63	1.332	1.44×10^{-8}
	1.61	1.317	0.87×10^{-4}
Ash	0.68	1.470	1.70×10^{-3}
	1.61	1.470	3.30×10^{-3}

Table 5: Refractive indices (n_r = real, n_i = imaginary) for water, ice and andesite. From Prata and Grant (2001).

At visible and near-infrared wavelengths scattering tends to dominate over absorption. The real and imaginary refractive indices of volcanic ash (andesite), water and ice give an indication of the strength of scattering and absorption, respectively. These are greatly affected by viewing geometry and particle size and shape. Prata and Grant (2001) studied the refractive indices (Table 5) for andesite, water and ice at approximately 0.6 μm and 1.6 μm and concluded that the ratio of the reflectances at these wavelengths could be used to distinguish ash clouds from water and ice clouds.

The real part of the refractive index is similar at 0.6 μm and 1.6 μm for ash, water and ice and so the scattering properties do not vary greatly between these wavelengths. The imaginary part of the refractive index does vary between 0.6 μm and 1.6 μm for water and ice but is similar for ash. In fact, the imaginary part of the refractive index is almost five orders of magnitude greater for volcanic ash than for water and ice at approximately 0.6 μm . By calculating the ratio of reflectances the effect of the viewing geometry is largely (but not entirely) eliminated.

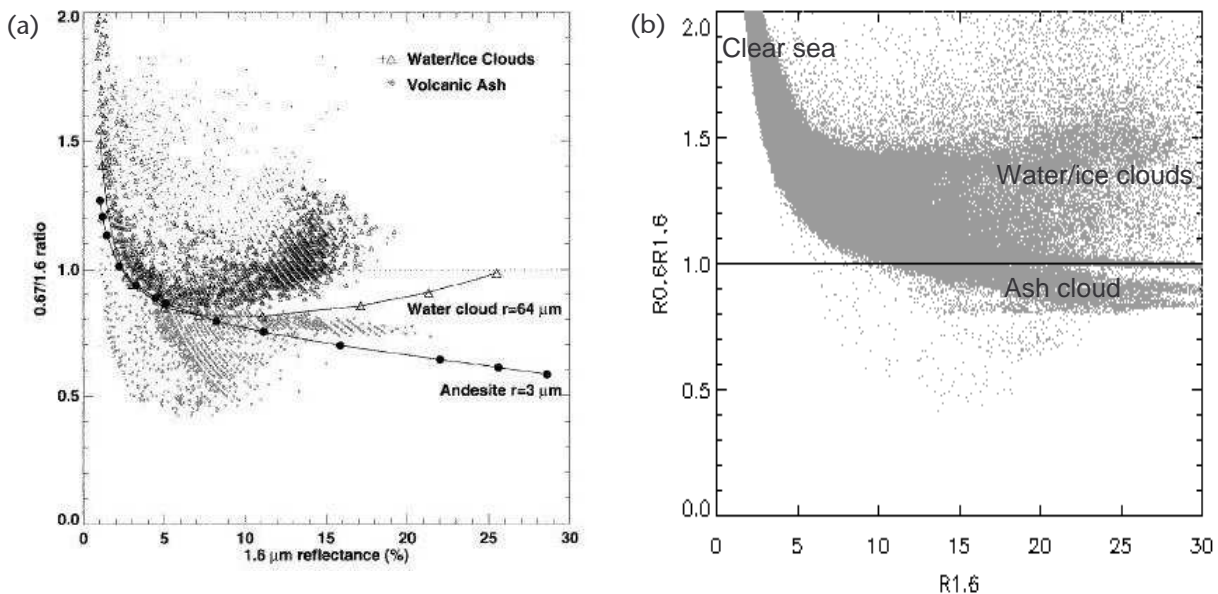


Figure 14: (a) Ratio of reflectances at 0.67 μm to 1.6 μm versus 1.6 μm reflectance for the volcanic ash plume from the 1996 Ruapehu eruption in New Zealand. From Prata and Grant (2001). (b) Corresponding scatter plot using Terra MODIS data for the eruption of Anatahan on 11 May 2003.

Prata and Grant (2001) used radiative transfer model calculations for a variety of viewing conditions based on the refractive indices in Table 5 and other properties described in their paper to show that the ratio of 0.67 μm to 1.6 μm reflectances can be used to discriminate ash from water and ice clouds. Discrimination is easiest at large optical depths. Figure 14(a) shows ATSR-2 R0.67/R1.6 values for the eruption cloud from

Ruapehu, New Zealand, on 8 July 1996 plotted along with the modelled values. This plot shows that the Ruapehu ash cloud produced ratios of between 0.5 and 0.8, whilst the water and ice clouds gave ratios of 0.8 to 1.4.

Due to the lack of instruments operating a channel in the near-infrared at 1.6 μm there has only been one other study on the application of data at this wavelength. This is by the Nowcasting SAF (LeGléau, 2001). They found that the ratio of reflectances does not discriminate well between volcanic ash and water and ice clouds. However, the method used to produce the plots does not allow for the selection of targets to be checked using subjective visual pattern recognition. Therefore, the selection of the targets used may not be accurately classified.

Volcano		Approximate measured R0.6 / R1.6 values
(a)	Hekla	0.8 to 1.2: Region of volcanic cloud 1.0 to 4.0: Water and ice clouds (mainly ice) 1.8 to 3.0: Clear sea
(b)	Cleveland	0.5 to 1.2: Volcanic cloud 1 to 3: Water/ice clouds 4 to 6: Clear sea
(c)	Etna	1.8 to 3.5: Volcanic cloud 2.0 to 4.0: Water clouds 8.0 to 18.0: Clear sea 0.4 to 0.8: Clear land
(d)	Anatahan	0.8 to 1.2: Volcanic cloud 1.2 to 2.0: Water/ice cloud 2.0 to 3.0: Clear seas
(e)	Grímsvötn	1.5 to 3.0: Volcanic cloud (contains a lot of water/ice) 1 to 3: Water/ice clouds 4 to 8: Clear sea
(f)	Anatahan	1 to 1.5: Volcanic cloud 1 to 3: Water/ice cloud 2 to 3: Clear sea

Table 6: Approximate observed signals in the imagery shown in Appendix E.

The examples studied here show R0.6/R1.6 values of 0.5 to 3.0 occur for volcanic clouds containing a mixture of ash, water vapour and other gases (Table 6). This overlaps with the signal seen for water and ice clouds and is similar in magnitude to the signal from cloud-free land. The Anatahan eruption in 2003 produced an ash cloud that resulted in R0.6/R1.6 values of 0.8 to 1.0 (Figure 14b), consistent with Prata and Grant (2001), whilst other eruptions produced volcanic clouds with higher ratios probably due to water and ice particles within the plume or viewing angle effects.

The clear sky values are highly variable; for example, the Mediterranean Sea shows R0.6/R1.6 values of 8 to 18. The ratio tends to vary with viewing geometry, both satellite and solar zenith angles (due to sun-glint); such that the smallest clear sky ratios are seen near nadir and the largest near the edge of the swath (Figure 15). This is the cause of the large ratios in the Etna image where the viewing angle near to the volcano is approximately 50°.

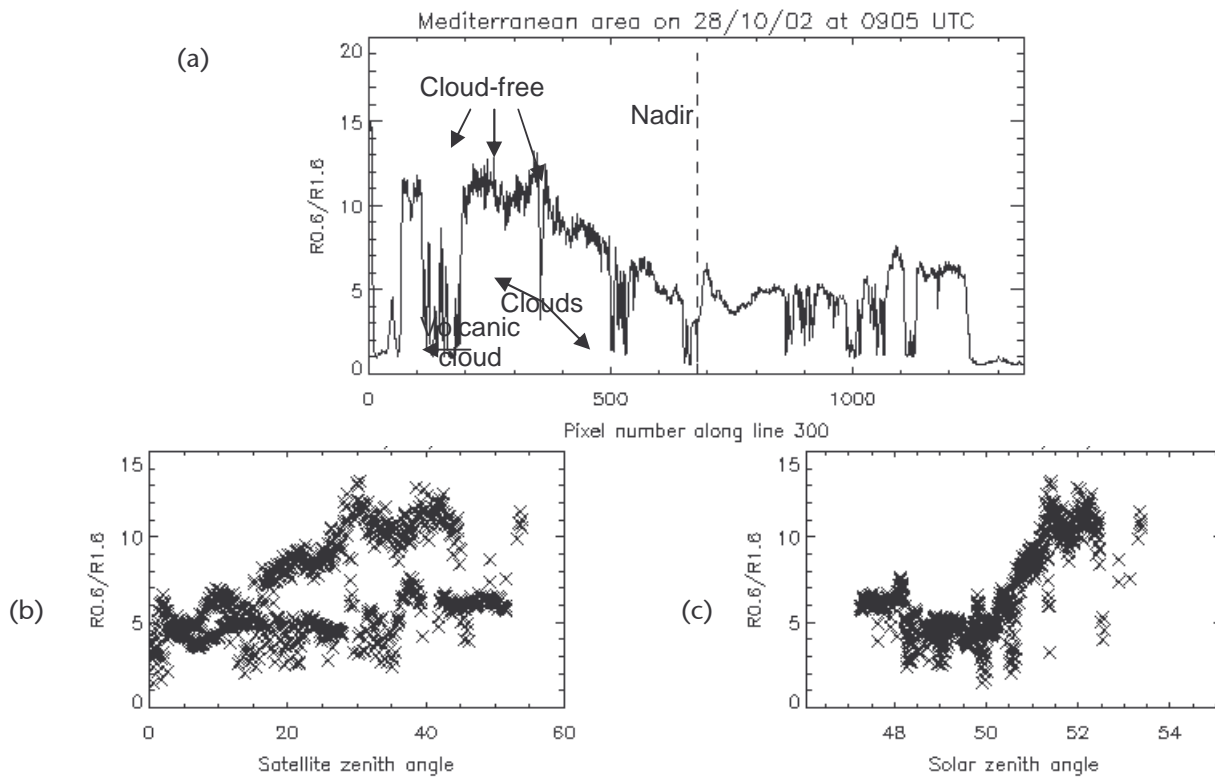


Figure 15: (a) A plot of a cross-section of $R0.6/R1.6$ values through the Mediterranean area on 28/10/02 at 0905 UTC. (b) and (c) the same data (with basic cloud screening) plotted against satellite zenith angle and solar zenith angle, respectively.

4.4. Visible RGB image

RGB (red-green-blue) images are a way of combining the information in three separate images without making any assumptions about the composition of the scene (e.g. without using threshold tests to isolate a component of the image). Each of the three images are scaled to 0-255 values and then assigned to a colour-gun.

The Visible RGB combines reflectances at 0.6, 0.8 and 1.6 μm in the following way:

- Red = 1.6 μm reflectance,
- Green = 0.8 μm reflectance, and
- Blue = 0.6 μm reflectance.

The colours in the resulting image are close to colours that the human eye would see. The image highlights surface features (vegetation (green) and desert (pink)), water cloud (white/pink) and ice cloud (cyan).

In general, volcanic ash clouds appear grey to white/pale pink because the reflectance is similar in the three channels. The variation is caused by variations in viewing geometry, plume composition and particle size.

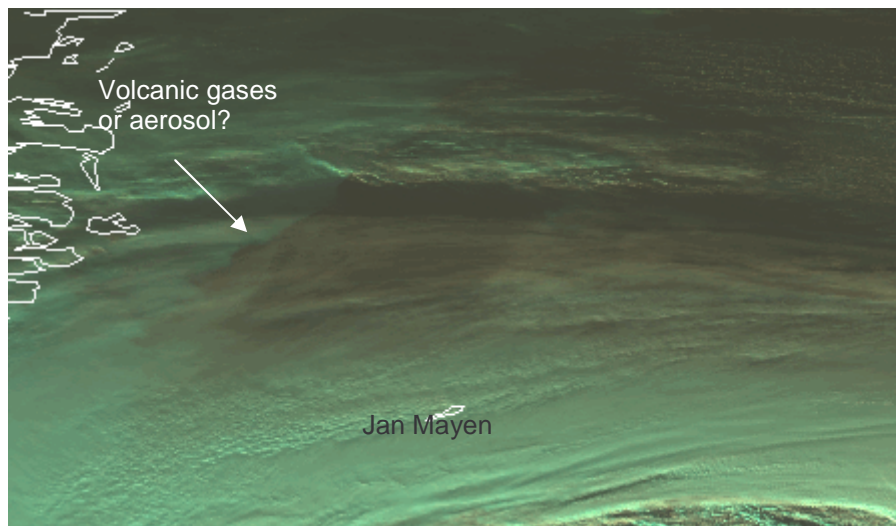


Figure 16: A MODIS Visible RGB image of the area north of Iceland during the eruption of Hekla on 27/02/00 at 1350 UTC.

The Visible RGB image of the Hekla eruption in February 2000 shows an area of low reflectance just north of Jan Mayen (Figure 18). This substance is overlying the layer of frontal ice cloud and corresponds to the area in which high sulphur dioxide concentrations were found (traced to originate from Hekla). It is not known what substance is causing the low reflectance values, whether volcanic gases or volcanic aerosol.

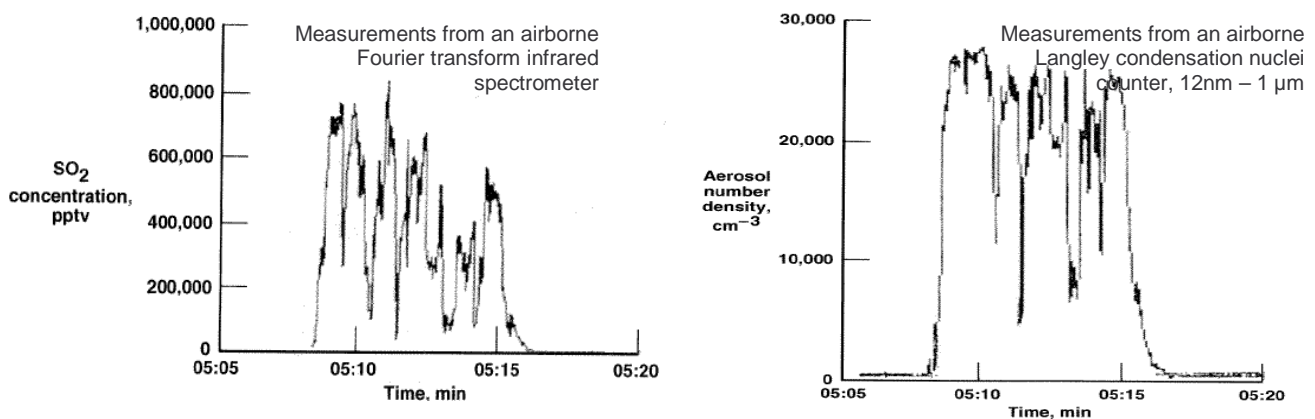


Figure 17: Sulphur dioxide and aerosol concentration measured on-board the NASA DC-8 aircraft as it flew through the volcanic plume from Hekla. From Gridle and Burcham (2003).

A NASA DC-8 aircraft on a SOLVE mission flew north of Iceland on 28 February. The highly-sensitive instruments detected high concentrations of sulphur dioxide and aerosols for seven minutes just after 0500 UTC as it encountered the volcanic cloud from Hekla (Figure 17). Additional data from the POAM instrument showed that there were high concentrations of gases and aerosol to cause high extinction rates at 1 μm in the lower stratosphere (Fig 18).

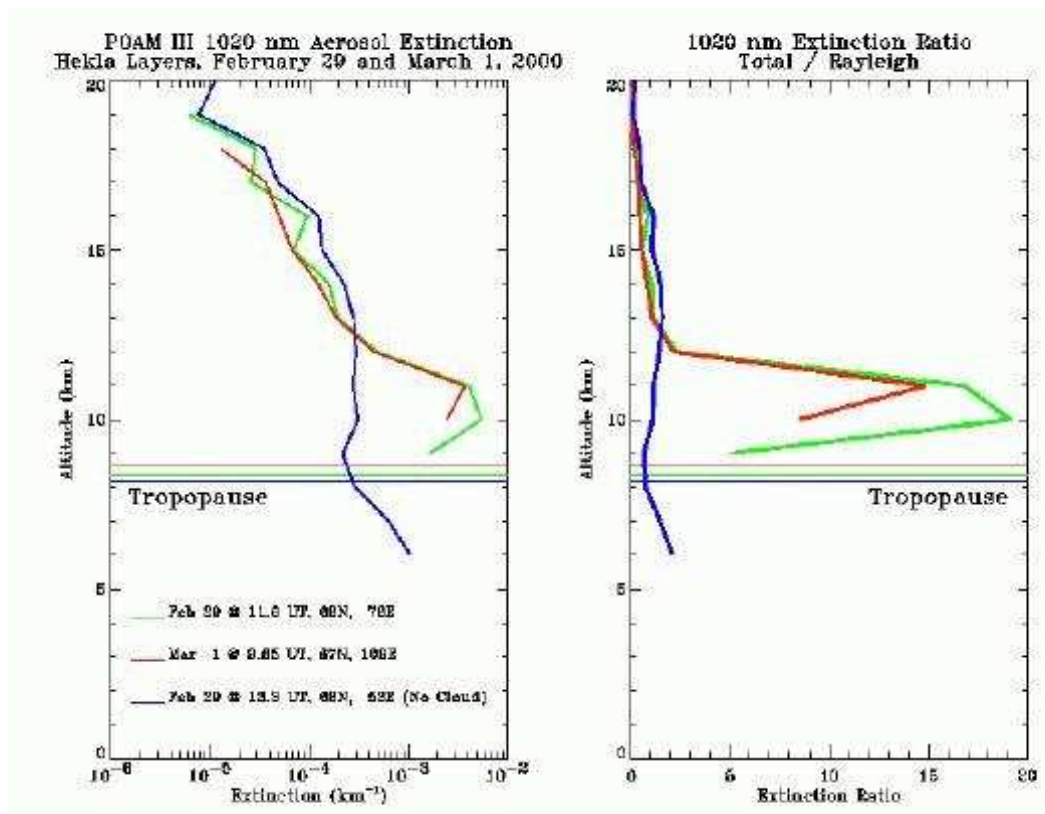


Figure 18: Polar Ozone and Aerosol Measurement (POAM) III aerosol and Rayleigh extinction profiles of the Hekla volcanic cloud from the Naval Research Laboratory.

4.5. Dust RGB image

The Dust RGB combines infrared brightness temperatures in the following way:

Red = $BT_{12.0} - BT_{10.8}$

Green = $BT_{10.8} - BT_{8.7}$

Blue = $BT_{10.8}$

The composition of dust and volcanic ash are similar: they are both silicates and therefore are radiometrically similar. Dust and ash result in a large red component (higher absorption at $10.8 \mu\text{m}$ than at $12.0 \mu\text{m}$), a small green component (greater absorption at $10.8 \mu\text{m}$ than at $8.7 \mu\text{m}$) and a mid to high blue component ($10.8 \mu\text{m}$ BT); thus dust and ash appear magenta in the Dust RGB images.



















Volcano	Volcanic plume			Clear sky		
(a) Hekla	 Region of volcanic gases					Thick cloud
(b) Cleveland	 Plume near volcano		Disperse plume			Opaque ice cloud
(c) Etna	 Volcanic plume					
(d) Anatahan	 Volcanic plume					
(e) Grímsvötn	 Volcanic plume		Water cloud			Opaque ice cloud
(f) Anatahan	 Volcanic plume					Water/ice cloud

Table 7: Approximate observed colours in the imagery shown in Appendix G.

The appearance of volcanic clouds in Dust RGB images is highly variable. The temperature profile has the largest effect on the resultant colours: high latitude, cold regions (e.g. Iceland and Alaska) display different colours (less blue) to low latitude, warm regions (e.g. Mediterranean and tropics).

4.6. Other volcanic ash detection tests

In addition to those above, several other channel combinations were studied. These are only mentioned here briefly to note their purpose and the results. However, they were not found to be as useful as those described in full above.

4.6.1. BT3.9 & BT10.8 or BT12.0

The 3.9 μm channel measures reflected solar and emitted terrestrial radiation. It is situated in an atmospheric window with fairly small amount of water vapour absorption. LeGléau (2001) found that at night BT3.9 – BT10.8 data could be used to discriminate volcanic ash from cloud-free areas and from water cloud. However, there is not a clear distinction between volcanic ash clouds and ice clouds. During the day, the distinction is less clear: the values for volcanic ash are similar to those for water and ice clouds.

In BT3.9 – BT12.0 images of the six eruptions in this study (not shown) all, except Grímsvötn, display high positive BTDs due to the high solar reflection at 3.9 μm (up to +50 K). In this respect the volcanic plume appears similar to meteorological clouds, particularly ice clouds. The Grímsvötn eruption produced a plume with low BTDs (approximately +10 K) due to low solar isolation.

4.6.2. Darwin VAAC BT10.8 – BT12.0 adjustment

The Darwin VAAC enhance the BT10.8 – BT12.0 image to reduce false alarms associated with high cloud tops by imposing a more negative threshold at very cold temperatures, such that:

$$\begin{aligned} T \geq 230 \text{ K}: & \quad T^* = \text{BTD} + c, \\ T < 230 \text{ K}: & \quad T^* = \text{BTD} + c + (230 - \text{BT10.8})/f, \end{aligned}$$

where f and c are empirically set values ($f = 12.5 \text{ K}$ and $c = 0$). The difference between BTD and T^* is generally small except in the tropics, where imagery was substantially improved through elimination of the false alarms associated with very cold cloud tops (Tupper et al., 2004). This adjustment was found to make negligible difference to the BT10.8 – BT12.0 images studied here and, as Tupper et al. (2004) conclude, the adjustment is only worth making in tropical locations.

4.6.3. Ellrod 3-channel algorithm

This test was developed for use with data from the GOES-12 imager, since this does not have the traditionally used split-window channels. Imagery at 10.8 and 13.4 microns has shown the ability to discriminate volcanic ash from ice-laden cirrus cloud layers due to emissivity differences (Ellrod et al., 2004). The algorithm is:

$$B = 5[(\text{BT3.9} - 1.5 \cdot \text{BT10.8} + 1.5 \cdot \text{BT13.4}) - 230]$$

Values between 230 and 300 are scaled to grey-scale values 0 to 255. Volcanic ash clouds produce high grey-scale values (typically larger than 150). The method has had mixed success in detecting ash from Soufriere Hills (failed on 12-13 July 2003, slight signal on 14 July 2004). It has also produced inconsistent results using MODIS imagery of the six eruptions in this study.

5. Conclusions and recommendations

The spectral signal of volcanic ash clouds is highly variable; it is dependent on the volcanic aerosols (e.g. composition, size, concentration, and altitude) and on the atmospheric conditions (cloud cover, water vapour content, temperature profile). A major problem is that volcanic eruptions are relatively rare events and so it is difficult to study a large sample in order to make conclusions about the spectral signature of these clouds in various conditions. However, this study of six diverse eruptions demonstrates the variability in the signals measured.

The split-window test (BT10.8 – BT12.0) is the most robust test and could be used to detect volcanic ash in five out of six of the eruptions. This should continue to be the main imagery used to monitor volcanic ash clouds. The graphical method for the adjustment of the BT10.8 – BT12.0 signal for water vapour absorption is useful in low-latitude locations. At high-latitude locations, the adjustment either makes little difference to the imagery (due to the low water vapour content), or the adjustment actually introduces false alarms. The factors affecting the BT10.8 – BT12.0 signal should be well understood in order to correctly interpret the observed signal. In particular, the limitations of the imagery should be made clear to forecasters, so that misdiagnosis of a potentially dangerous situation does not occur.

Additional imagery can aid the interpretation of the situation. The most useful imagery identified in this study is the RGB images. The Visible RGB can be used to clarify the meteorological situation (presence of ice clouds etc.) as well as monitoring the volcanic plume. Dust RGB images are actually useful for identifying that the volcanic plume contains ash and is particularly useful for monitoring ash clouds in warm climates. The BT10.8 – BT8.7 imagery highlights the volcanic plume, but the signal can be confusing. It is thought that much of the signal seen in this imagery is actually from sulphur dioxide or sulphuric acid absorption. The 8.7 μm channel may prove useful (when used in conjunction with other channels) to assess the composition of a volcanic plume. Further work on the application of MSG data for sulphur dioxide monitoring will help to clarify the cause of the signals in this imagery. It is recommended that the Visible and Dust RGB images are made operationally available for areas of volcanic ash monitoring.

Most of this study was conducted using MODIS data, simply because the library of SEVIRI data is not yet large enough to contain a sufficient number of volcanic eruptions. The main difference between the data from these two instruments is in the temporal and spatial resolutions. The relatively coarse resolution of SEVIRI imagery (3km at nadir, up to 11 km over Iceland) is compensated, in part, by the rapid repeat cycle, every 15 minutes. This enables some very beneficial animations to be created that forecasters can use to identify clouds that are not easy to identify in a static image. However, the high spatial resolution of MODIS data means that small-scale features can be identified that are missed in the SEVIRI imagery. There are approximately eight passes per day from polar orbiter platforms that carry MODIS (i.e. Terra and Aqua) over Iceland. Real-time MODIS imagery of the Icelandic area would be highly beneficial for the London VAAC service. These data are routinely received at the Met Office in Exeter, but are not yet processed. It is recommended that multi-channel imagery is developed using MODIS data for volcanic ash monitoring over and near Iceland.

The EOS (Earth Observing System) satellites (Terra and Aqua) that carry MODIS are only designed for a six-year lifetime. There are no plans to replace the MODIS instruments directly. However, the VIIRS (Visible Infrared Imager / Radiometer Suite) has channels that are similar to those on MODIS. This instrument will be carried on the NPP and NPOESS missions from 2008, so that any monitoring imagery developed for MODIS will be able to be produced using VIIRS data in the future.

During the course of this project (Sept 2004 – July 2005) there has only been one volcanic eruption within the Meteosat-8 field-of-view. The eruption of Grímsvötn was difficult to monitor due to the large amount of frontal cloud in the area. The particles in the volcanic plume became coated in ice, and so an ash signal could not be observed in the MODIS or SEVIRI imagery, except very close to the volcano. This eruption, whilst being an important case study, did not prove a useful example to test the multi-channel imagery due to the complexity of the scene and the composition of the volcanic plume. The multi-channel imagery should continue to be tested on any future eruptions within the Meteosat-8 field-of-view to compare the performance of MODIS and SEVIRI imagery and to gain further experience of observing volcanic signals in the imagery.

References

- Baran, A.J., Foot, J.S. and Dibben, P.C., 1993. Satellite detection of volcanic sulphuric acid aerosol. *Geophysical Research Letters*, **20**, 1799-1801.
- Dean, K.G., Dehn, J., Papp, K.R., Smith, S., Izbekov, P., Peterson, R., Kearney, C. and Steffke, A., 2004. Integrated satellite observations of the 2001 eruption of Mt. Cleveland, Alaska. *Journal of Volcanology and Geothermal Research*, **135**, 51-73.
- Ellrod, G. P., and Jung-Sun, Im, 2003. Development of volcanic ash products using MODIS multi-spectral data. *AMS Conference on Satellite Meteorology and Oceanography*, 12, Long Beach, CA, 9-13 February 2003.
- Gridle, T.J., and Burcham, F.W., 2003: Engine damage to a NASA DC-8-72 airplane from a high-altitude encounter with a diffuse volcanic ash cloud. *NASA Technical Memorandum* (NASA/TM-2003-212030).
- Guffanti, M., Casadevall, T.J., and Mayberry, G.C., 2004. Reducing encounters of aircraft with volcanic ash clouds. *Proceedings of the 2nd International Conference on Volcanic Ash and Aviation Safety*, Session 1, p. 17, Washington, June 2004.s
- Le Gléau , H, 2001. Use of MODIS to enhance the PGE01-02 of SAFNWC/MSG. *NWC SAF*. March 2002.
- Prata, A.J. and Grant, I.F. (2001). Retrieval of microphysical and morphological properties of volcanic ash plumes from satellite data: Application to Mt Ruapehu, New Zealand. *QJRM*, 127, 2153 - 2179
- Prata, A. J. (1989). Observations of volcanic ash clouds in the 10-12 μ m window using AVHRR/2 data. *International Journal of Remote Sensing*, 10, 751-761.
- Smithsonian Institute, Global Volcanism Program: <http://www.volcano.si.edu/>
- Tupper, A., Carn, S., Davey, J., Kamada, Y., Potts, R., Prata, F. and Tokuno, M, 2004. An evaluation of volcanic cloud detection techniques during recent significant eruptions in the western 'Ring of Fire'. *Journal of Volcanology and Geothermal Research*, **135**, 27-46.
- Watkin, S.C., 2001. A description of an AVHRR volcanic ash detection product and examples of its application. *Met Office NWP Technical Report*, No. 358.
- Watkin, S.C., 2003. The application of AVHRR data for the detection of volcanic ash in a Volcanic Ash Advisory Centre. *Meteorological Applications*, **10**, 301-311.
- Watson, I.M., Realmuto, V.J., Rose, W.I., Prata, A.J., Bluth, G.J.S., Gu, Y., Bader, C.E. and Yu, T. 2004. Thermal infrared remote sensing of volcanic emissions using the moderate resolution imaging spectroradiometer. *Journal of Volcanology and Geothermal Research*, **135**, 75-89.

Acknowledgments

Roger Saunders generated the RTTOV clear sky simulations shown in Figures 11a and 11b and provided valuable advice during this project.

Roger Saunders and John Eyre reviewed this report provided useful comments and corrections.

Acronyms

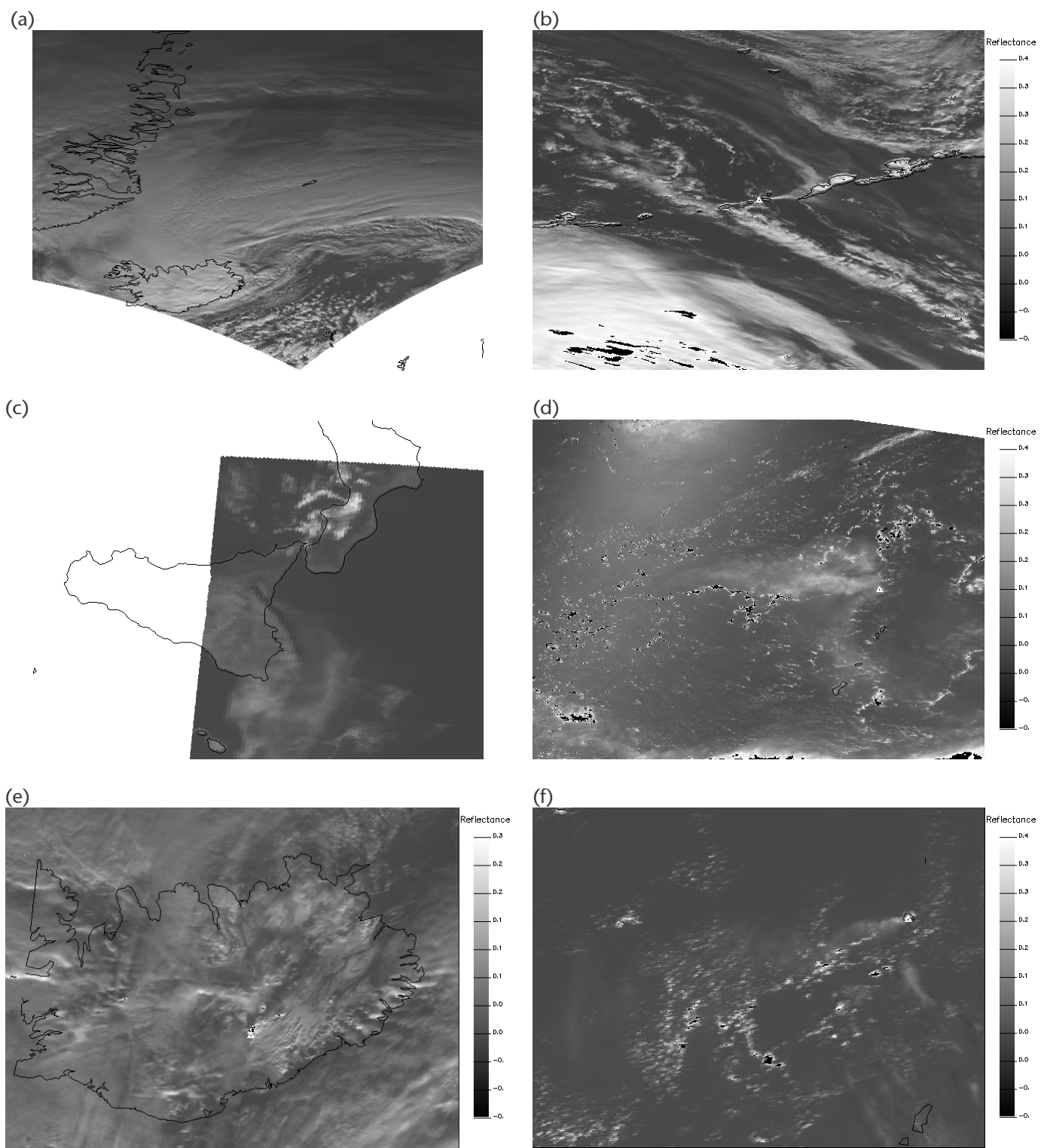
ATSR	Advanced Tracking Scanning Radiometer
AVHRR	Advanced Very High Resolution Radiometer
BT	Brightness temperature
BTD	Brightness temperature difference
EMARC	Environment Monitoring and Response Centre
GOES	Geostationary Operational Environmental Satellite
HIRS	High resolution Infra-Red Sounder
MODIS	Moderate resolution imaging spectroradiometer
MSG	Meteosat Second Generation
NAME	Nuclear Accident Model (Atmospheric dispersion model)
NOAA	National Oceanic and Atmospheric Administration
POAM	Polar Ozone and Aerosol Measurement
R	Reflectance
RGB	Red-green-blue
SAF	Satellite Application Facility
SEVIRI	Spinning Enhanced Visible and Infrared Imager
TOMS	Total Ozone Mapping Spectrometer
UTC	Universal Time Coordinate
VAAC	Volcanic Ash Advisory Centre

Appendices

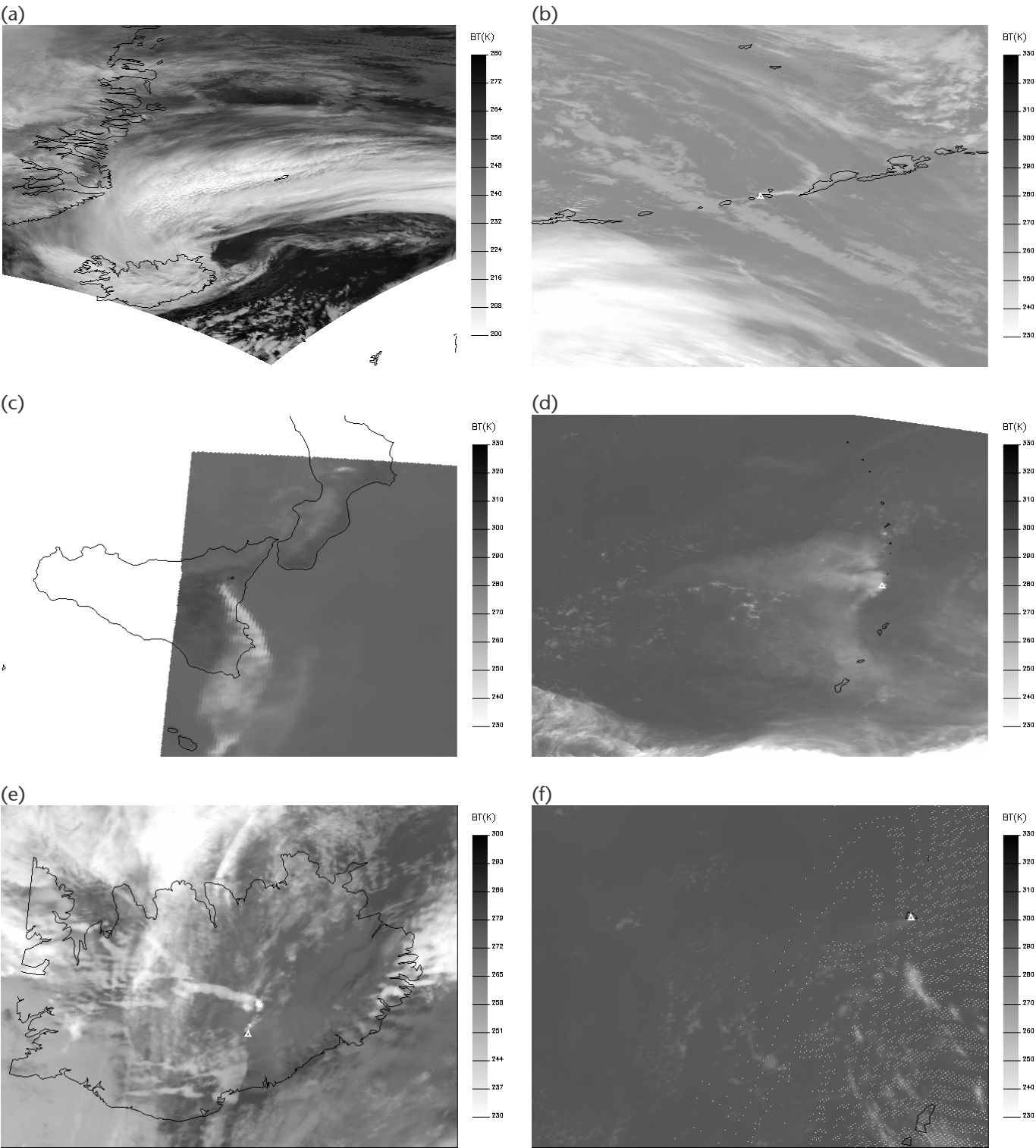
Label	Volcano	Location	Date and time of imagery
(a)	Hekla	Iceland	27/02/2000 1350 UTC
(b)	Cleveland	Alaska, USA	19/02/2001 2310 UTC
(c)	Etna	Sicily, Italy	28/10/2002 0905 UTC
(d)	Anatahan	Marianas Is.	11/05/2003 0125 UTC
(e)	Grímsvötn	Iceland	02/11/2004 1210 UTC
(f)	Anatahan	Marianas Is.	11/02/2005 0110 UTC

MODIS data for the six eruptions described above were used to study the various detection tests. The table above lists the date and time of the MODIS used for each of the eruptions. All the imagery is during daylight hours. In all the images the white triangle marks the location of the volcano.

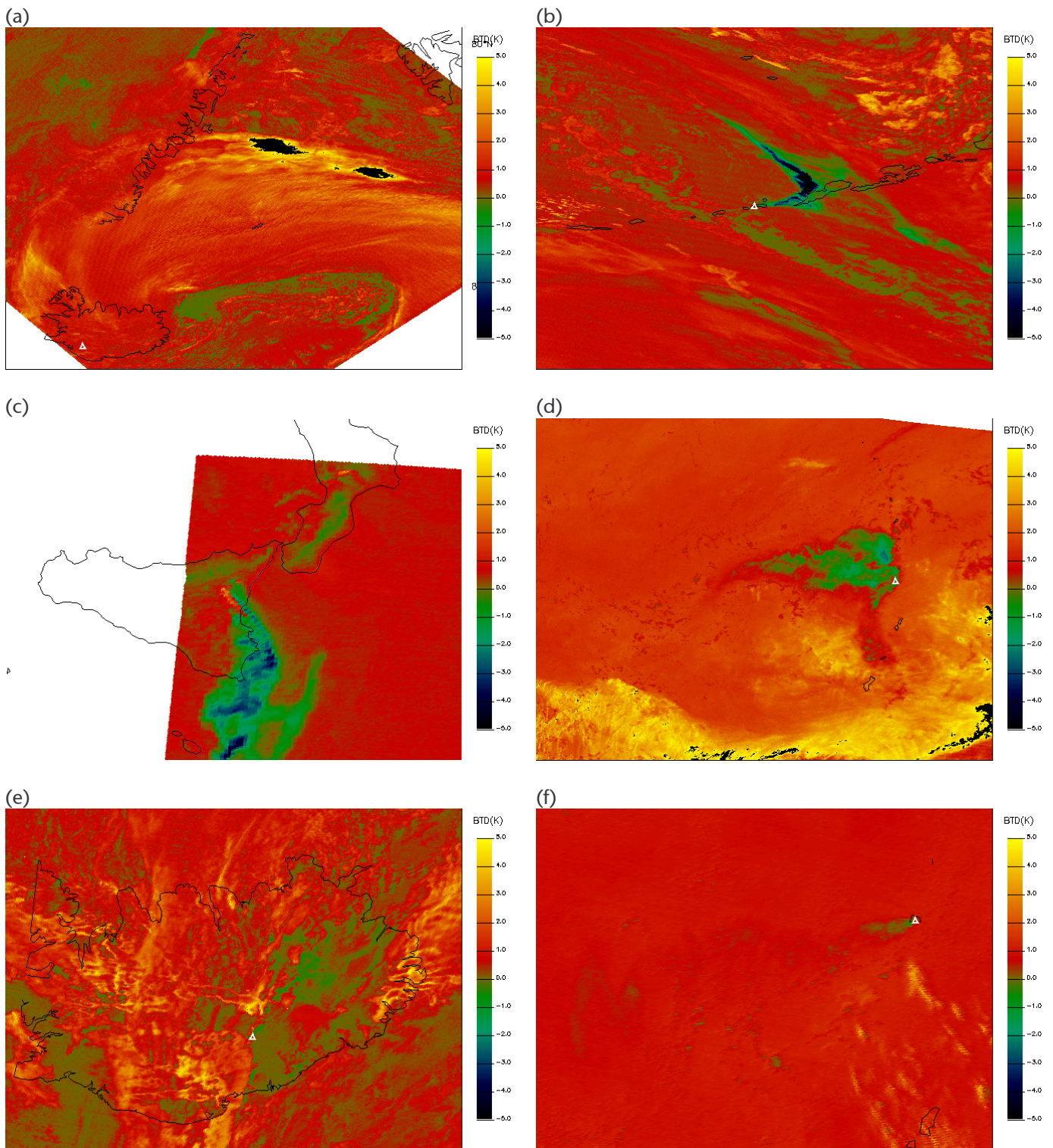
Appendix A: 0.6 μm reflectance for eruption clouds (a) to (f)



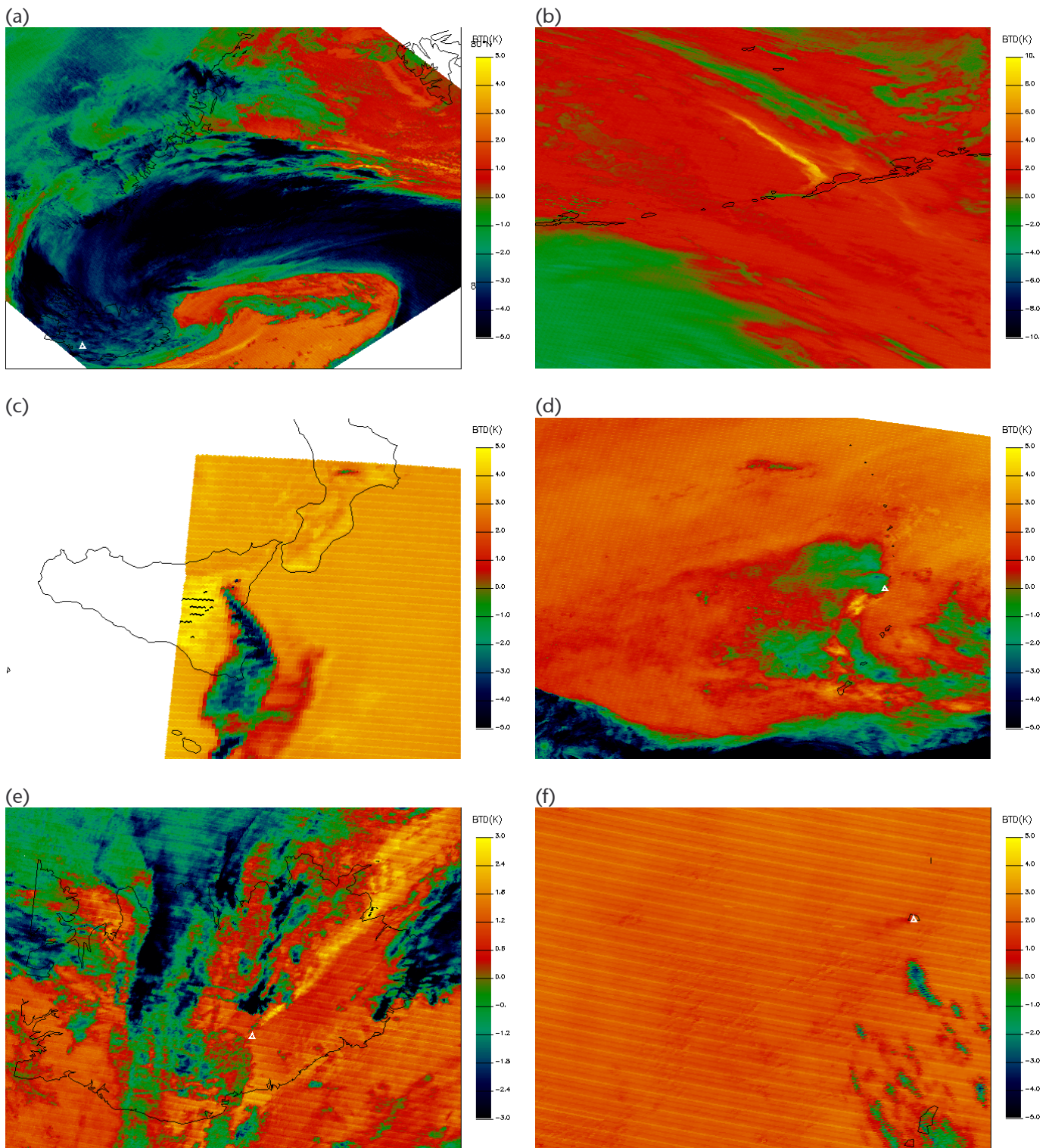
Appendix B: BT10.8 for eruption clouds (a) to (f)



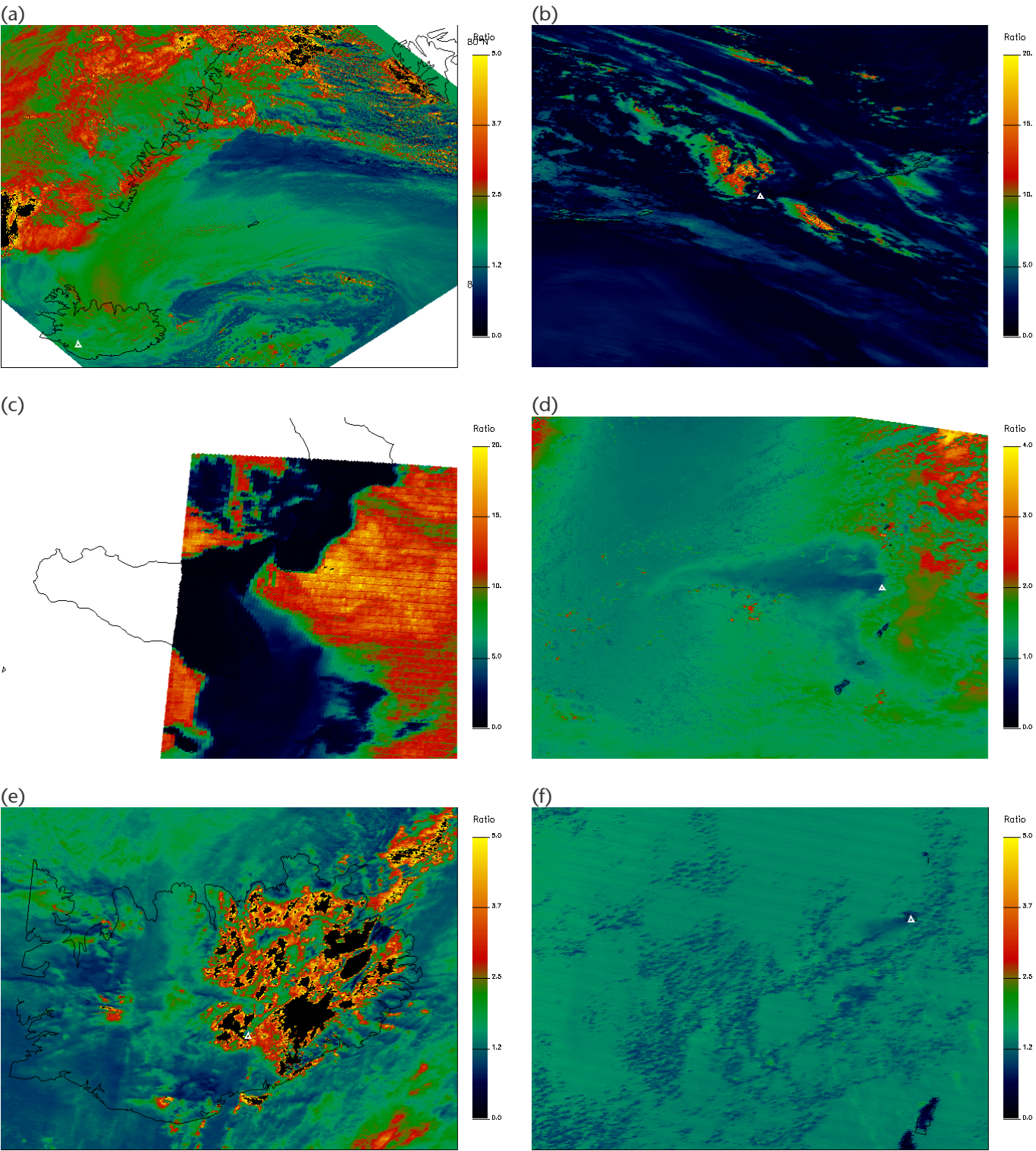
Appendix C: BT10.8 – BT12.0 for eruption clouds (a) to (f)



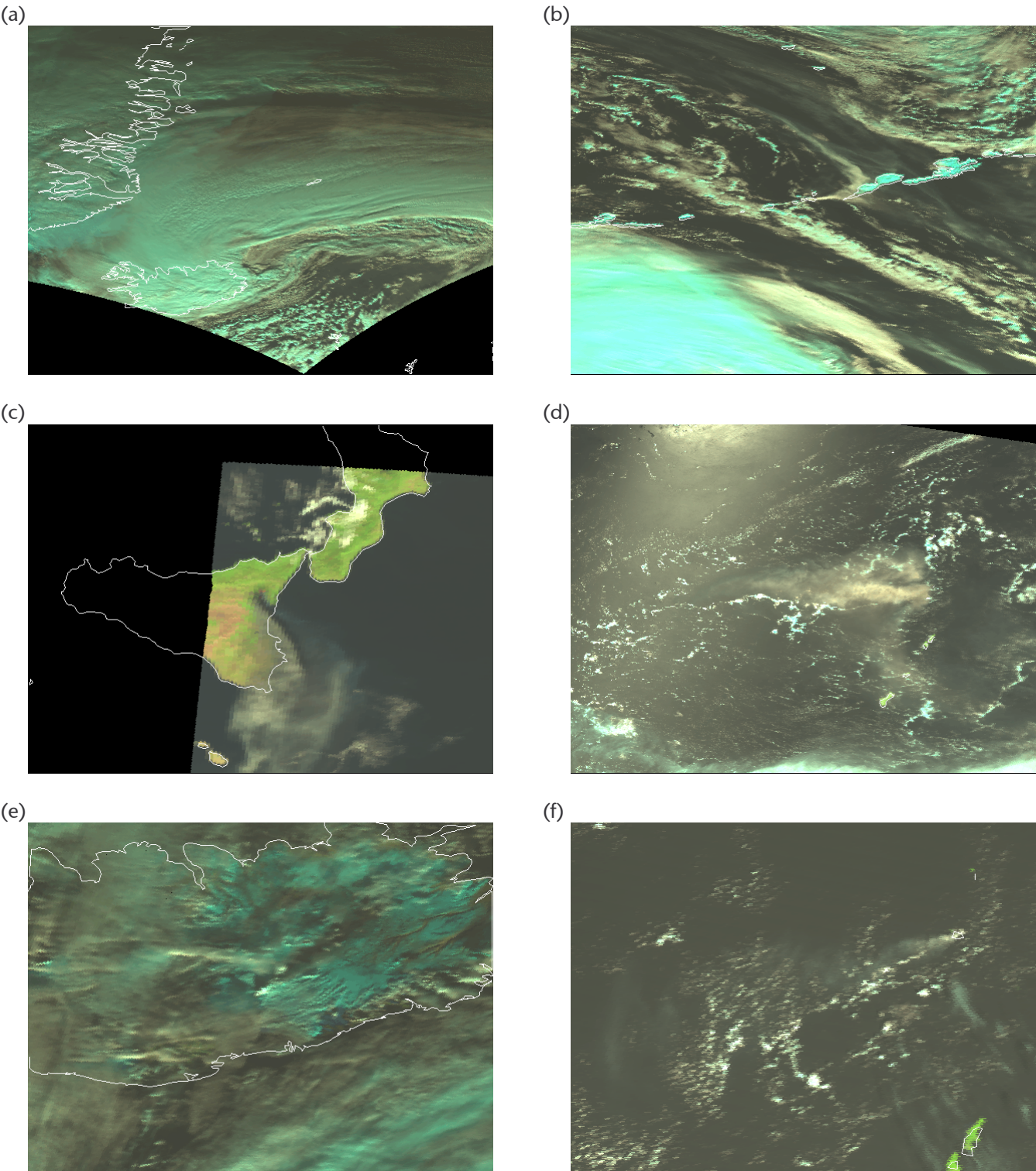
Appendix D: BT10.8 – BT8.7 for eruption clouds (a) to (f)



Appendix E: R0.6/R1.6 for eruption clouds (a) to (f)



Appendix F: Visible RGB for eruption clouds (a) to (f)



Appendix G: Dust RGB for eruption clouds (a) to (f)

